SLAC-PUB-12310
Astronical Journal, submitted
January 2007
Preprint typeset using LaTeX style emulateapj v. 25/04/01

FIRST 'WINGED' AND 'X'-SHAPED RADIO SOURCE CANDIDATES

C. C. Cheung[1]
National Radio Astronomy Observatory; and
Kavli Institute for Particle Astrophysics and Cosmology, Stanford University, Stanford CA 94305
teddy3c@stanford.edu
Astronical Journal, submitted

ABSTRACT

A small number of double-lobed radio galaxies (17 from our own census of the literature) show an additional pair of low surface brightness 'wings', thus forming an overall 'X'-shaped appearance. The origin of the wings in these radio sources is unclear. They may be the result of back-flowing plasma from the currently active radio lobes into an asymmetric medium surrounding the active nucleus, which would make these ideal systems in which to study thermal/non-thermal plasma interactions in extragalactic radio sources. Another possibility is that the wings are the aging radio lobes left over after a (rapid) realignment of the central supermassive black-hole/accretion disk system due perhaps to a merger. Generally, these models are not well tested; with the small number of known examples, previous works focused on detailed case studies of selected sources with little attempt at a systematic study of a large sample. Using the VLA-FIRST survey database, we are compiling a large sample of winged and X-shaped radio sources for such studies. As a first step toward this goal, an initial sample of 100 new candidate objects of this type are presented in this paper. The search process is described, optical identifications from available literature data, and basic radio data are presented. From the limited resolution FIRST images ($\sim 5''$), we can already confidently classify a sufficient number of these objects as having the characteristic wing lengths >80% of the active lobes to more than double the number of known X-shaped radio sources. We have also included as candidates, radio sources with shorter wings (<80% wing to lobe length ratios), or simply 'winged' sources, as it is probable that projection effects are important. Finally, among the candidates are four quasars (z=0.37 to 0.84), and several have morphologies suggestive of Fanaroff-Riley type-I (low-power) radio galaxies. While followup observations are necessary to confirm these identifications, this stresses the importance of source orientation and imaging limitations in finding these enigmatic objects.

Subject headings: Galaxies: active — galaxies: jets — quasars: general — radio continuum: galaxies

1. BACKGROUND AND MOTIVATION

'Winged', or 'X'-shaped radio galaxies form a small and interesting subclass of extragalactic radio sources (e.g., Leahy & Parma 1992; Dennett-Thorpe et al. 2002). In addition to the usual pair of 'active' lobes, these objects possess an additional pair of lower surface brightness 'wings' of emission, thus forming an overall winged or X-shaped appearance (see Figure A1 for examples).

There is no clear explanation for the origin of these unusual morphologies. One possibility is that the wings result from back-flow (Leahy & Williams 1984) of plasma from the "working surfaces" (hot spots) in the active lobes into an asymmetric surrounding medium, with subsequent buoyant expansion (Worrall et al. 1995). In this scenario, it has been argued that the expansion of the wings is subsonic and it becomes difficult to explain sources with wings that are longer than the active lobes (Dennett-Thorpe et al. 2002). However, this supposes that the active lobes are expanding supersonically, and into a roughly spherically symmetric medium – neither assumption may be applicable to these objects (Capetti et al. 2002; Kraft et al. 2005).

Another explanation that has received much attention lately is that the wings are the remnant left over from a rapid realignment of a central supermassive black hole/accretion disk system (e.g., Dennett-Thorpe et al. 2002), perhaps due to a relatively recent merger of a binary supermassive black-hole (SMBH) system (e.g., Rottmann 2001; Merritt & Ekers 2002; Gopal-Krishna et al. 2003; Zier 2005). The X-sources are then one of only a few observational systems attributable to SMBH binaries (Komossa 2003). In this respect, a census of these sources is important to estimate the occurrence rate of mergers (e.g., Merritt & Ekers 2002; Hughes & Blandford 2003) and recurrence time-scales of (radio-loud) active galaxies (e.g., Liu 2004).

One major obstacle in understanding the origin of the X-shaped radio sources as a class is that there are only a small number of known examples – 17 in total from our own census of the literature (Table A1), though wings in radio galaxies are fairly common (§ 2). It is unclear whether these known ones are representative of the class as a whole. They are in the majority, identified in imaging surveys of radio samples with high flux density thresholds (§ 5.2). This may explain their limited range of properties: the well-known examples are relatively local (within z<0.3), and the radio luminosities straddle the Fanaroff-Riley (FR) division (Fanaroff & Riley 1974), with a dearth of sources showing FR-I morphology (Dennett-Thorpe et al. 2002). Of these, only a handful have been studied in sufficient detail to compare to the differing model expectations (Worrall et al. 1995; Ulrich & Roennback 1996; Dennett-Thorpe et al. 2002; Kraft et al. 2005). Until only

[1] Jansky Postdoctoral Fellow

Work supported in part by the US Department of Energy contract DE-AC02-76SF00515

recently (§ 5.1; Wang et al. 2003; Landt et al. 2006), none showed broad-emission lines characteristic of quasars (i.e., the population of radio galaxies aligned close to our line of sight), stressing the importance of source orientation in identifying new examples (§ 5.3).

We can begin to address these issues by using larger radio imaging surveys to search for more examples of X-sources to expand the current sample for follow-up studies. We are carrying out such a project in search of new winged and X-shaped radio sources using the FIRST (Faint Images of the Radio Sky at Twenty-centimeters) survey (Becker et al. 1995) (§ 3). Our simple search procedure, described here, and applied to a subset of the FIRST database, resulted so far in 100 radio sources we propose as candidates (§§ 3 and 4). Although there are already a sufficient number of clear new examples of bona-fide X-shaped radio sources to at least double the known sample, the majority require higher resolution and better sensitivity observations to map out their morphologies more clearly (Figure A1). We have included sources with shorter wings (canonically, <80% lobe length; Leahy & Parma 1992) with the hopes of disentangling projection effects. As part of the search process, we have compiled an up-to-date catalog of known X-shaped radio sources from the literature which is used to evaluate the success of our search methods (§ 5). A summary is given in § 6.

Throughout this paper, we assume a ΛCDM cosmology with parameters $h = H_0/(100 \text{ km s}^{-1} \text{ Mpc}^{-1}) = 0.7$, $\Omega_M = 0.3$ and $\Omega_\Lambda = 0.7$.

2. DEFINITION AND CENSUS

As part of our search for new examples, we compiled a list of winged and X-shaped radio sources commonly discussed in the literature (Table A1). Fourteen well-known examples are listed by Rottmann (2001), Capetti et al. (2002), and Merritt & Ekers (2002) (attributed to Leahy & Parma (1992)). The X-shaped nature of the radio source 4C+04.40 (Junor et al. 2000) was revealed contemporaneously to these works. Wang et al. (2003) recently reported 4C+01.30 as the first X-shaped source with a quasar nucleus (i.e the population of radio galaxies with the main axis aligned closer to our line-of-sight), showing broad emission lines in its spectrum. One more quasar has since been identified as an X-shaped radio source (Landt et al. 2006), and we located two additional, more distant ($z \sim 0.4$; Lehár et al. 2001; Zakamska et al. 2004) X-shaped radio galaxies in published maps. See the Appendix for notes on these five additional examples from the literature.

The known examples show a range of wing to lobe length ratios (in projection). This brings up the issue of nomenclature and the characteristics distinguishing an X-shaped source from a winged one. Conventionally, winged radio sources with the most extended wings (>80% of the extent of the lobes; Leahy & Parma 1992) are called X-shaped, but these are clearly phenomenologically related to shorter winged objects. The radio galaxy 4C+32.25 shows the most prominent wings, being just over a factor of two more extended than its lobes. 3C 192 and 3C 379.1 have the shortest wings (∼65% of extent of lobes; Dennett-Thorpe et al. 1999; Spangler & Sakurai 1985, respectively), so by convention, do not qualify as being X-shaped. However, the wings in the latter two examples may appear shortened by projection, or they may be caught in a stage of early growth or later decay (see § 5.3). It is apparent that such effects should be accommodated in further discussions of these objects as a class.

The present search aims to identify new X-shaped radio sources, and winged ones are included with the points above in mind. In fact, wings are quite commonly seen in deep radio images of 3CR radio galaxies (e.g., Leahy & Williams 1984; Leahy & Perley 1991), but we will not attempt to catalog them all here. Deeper observations of our candidates should determine the true extent of the wings where they may not be so apparent in the limited sensitivity FIRST survey finder images. For these reasons, we use winged and X-shaped interchangeably throughout the rest of the text.

3. IDENTIFYING NEW WINGED AND X-SHAPED RADIO SOURCE CANDIDATES WITH FIRST

The FIRST survey uses the NRAO[2] Very Large Array (VLA) at a wavelength of 20cm (1.4 GHz) to image the radio sky with an angular resolution of $\sim 5''$ (Becker et al. 1995). This relatively high resolution and the good sensitivity achieved in the survey images (typical rms of 0.13 mJy) has allowed investigations of new fainter samples of morphologically distinct radio sources such as, compact steep spectrum (CSS; Kunert et al. 2002), hybrid morphology (with FR-I and II characteristics; Gawronski et al. 2006), and core-dominated triples (Marecki et al. 2006). Here, we are similarly exploiting this unique database to search for new examples of X-shaped radio sources.

One of the main survey products is a catalog of radio "sources" derived from fitting 2-dimensional Gaussians (with deconvolved major and minor axes, *maj.* and *min.*, respectively, and fitted peak flux) to the images. By virtue of the high angular resolution of the survey, many of these sources are often the separate components in a single object decomposed, e.g. the lobes and/or hot spots in a double-lobed radio galaxy. Most are simply unresolved point sources, or attempts by the software to fit more complicated source structures with a single Gaussian when they were inadequately resolved – see Proctor (2003, 2006) for a discussion.

This catalog of radio sources can be queried through the search engine on the FIRST website (http://sundog.stsci.edu/). We ignored sources flagged by the software as sidelobes due to a nearby bright source. The latest data release (2003 April 11)[3] was utilized; the sky coverage in this version of the catalog is approximately 8422 deg^2 in the north galactic cap (7.0 hr<R.A.<17.5 hr, −8.0 deg<Dec.<+57.6 deg), and 611 deg^2 in the south galactic cap (21.3 hr<R.A.<3.3 hr, −11.5 deg<Dec.<+1.6 deg). The current FIRST catalog contains ∼811,000 sources (footnote 3).

3.1. *FIRST Search Procedure*

[2] The National Radio Astronomy Observatory is operated by Associated Universities, Inc. under a cooperative agreement with the National Science Foundation.

[3] http://sundog.stsci.edu/first/catalogs/readme_03apr11.html

With the large number of images fields provided by FIRST, our strategy is to visually examine only a well-defined subset of these:

- fields with sufficient dynamic range (defined as the ratio of the peak : rms) in the images to be able to see extended low surface brightness wings, and
- those containing sources with resolved structure easily discernible with the $\sim 5''$ resolution of the survey.

These two issues are discussed in turn.

With a given image sensitivity, it becomes increasingly difficult to distinguish the morphology of a low image peaked radio source by-eye (below a few mJy/bm in FIRST). For X-shaped sources, the surface brightness of the wings are typically much lower than the brighter active lobes/hot spots (the usual brightest parts of a radio galaxy). Quantitatively, low-peaked fields of X-sources yield at most, only a few sigma detections of possible wing emission. In this work, we determined that fields with image peaks of 5 mJy/bm and greater ($\sim$40:1 dynamic range) worked reasonably well enough (§ 5.1) to see the extended emission and set this as the limit in our queries.

Ideally, we would have liked to inspect every field containing at least one resolved source indicating the presence of an extended lobe. This can be done by setting both *maj.* and *min.*$>5''$, the resolution of the FIRST images. However, setting this along with the >5 mJy/bm image peak limit returned a large number of sources (8,146), with a small percentage in overlapping fields whenever more than one component in the field matched the search criteria. (For reference, setting a twice fainter peak level returned approximately double the fields in our queries.) For this initial phase of our project, we relaxed the fitted major axis to *maj.*$>15''$ which returned a much more manageable 1,648 source fields for visual inspection. We hope to address the remaining fields in future iterations.

Our queries returned color GIF images of the 5×5 arcmin^2 FIRST fields which we inspected by-eye and downloaded the FITS images of the fields with hints of extended structure characteristic of wings. The FITS images were then further scrutinized using the SAOImage-ds9 interface to control the contrast in the images. A working list of candidates was generated for optical identifications with rough positions estimated from the radio morphologies, usually where the radio lobes intersect when a central source was not present. The final list of candidates were judged to show at least one wing roughly orthogonal to a pair of active lobes.

3.2. *Optical Identifications and Properties*

We cross-referenced our radio-based estimated positions with NED[4], the Digital Sky Survey (DSS) based USNO-B1.0[5] (Monet et al. 2003), and APM (Maddox et al. 1990; McMahon et al. 2002) catalogues, and the Sloan Digital Sky Survey[6] (SDSS). The identifications were based on the position of the optical object relative to the radio source morphology. This was aided by making radio/optical overlays of the fields using the FIRST and red-filter DSS images (Figure A4). Known X-shaped sources (§ 5) were identified and removed from the candidate list.

For the objects without catalogued or visible optical counterparts (6 cases), we kept the best guess radio-morphology based positions; these are less precise because the radio emission is extended. An (uncatalogued) smudge appears near the radio-predicted position of J1655+4551 in the DSS red image – we made a by-eye position measurement of this optical source.

Of the 100 candidates, 36 are spectroscopically identified, with half of them (18/36) found in the latest SDSS data release (DR5; Adelman-McCarthy et al. 2007). This is no surprise, as the FIRST survey was designed to have overlapping coverage with the SDSS. One new identification was obtained for us by S.E. Healey (2005, private communication) observing at the MacDonald Observatory (J0702+5002; see notes in § 4). The remaining spectroscopic identifications are from prior work found in the literature; three of these have SDSS data confirming their IDs. The positions, optical (SDSS or POSS-II) r-band magnitudes, $g-r$ colors of the SDSS identified objects, and spectroscopic identifications & redshifts for the 100 final candidates are tabulated in Table A2.

Among the 36 spectroscopically identified candidates are four quasars; the remainder are radio galaxies. The quasars were identified by the SDSS as having at least one broad (>1000 km s^{-1}) emission line (Schneider et al. 2002). The three highest redshift (z>0.5) quasars have bluer colors ($g-r$=–0.1 to 0.2), indicative of a quasar nucleus dominating the optical continuum. The fourth quasar (J1430+5217), at a more modest redshift of z=0.367, has the clearest winged appearance among the quartet (Figure 1), although curiously has a redder color ($g-r$=1.1) more like the radio galaxies. The unidentified J1406+0657 ($g-r$=0.0) and to a lesser degree, J1342+2547 ($g-r$=0.4), are bluer like the highest redshift quasars; spectroscopic observations are necessary to determine if they are quasars also. Other higher redshift candidates of note are the radio galaxies J0143–0119 (z=0.52), J0115–0000, J0941–0143, and J1309–0012 (latter three are at $z\sim$0.4).

Figure A4 shows the fields of the 100 candidate X-shaped sources in the radio (FIRST) and the optical (Digital Sky Survey red images) centered on the best determined positions. Each field is 2×2 arcmin^2, except for the cases of the two largest angular size radio sources (J0113+0106 and J1424+2627) where larger 4×4 arcmin^2 fields are displayed. Thumbnail color versions of the FIRST images which emphasize the diffuse emission are shown in Figure A1. Notes on each candidate are provided in § 4.

[4] This research has made use of the NASA/IPAC Extragalactic Database which is operated by the Jet Propulsion Laboratory, California Institute of Technology, under contract with the NASA.

[5] This research has made use of the USNOFS Image and Catalogue Archive operated by the United States Naval Observatory, Flagstaff Station (http://www.nofs.navy.mil/data/fchpix/); the "-B1.0" is suppressed hereafter.

[6] Funding for the SDSS and SDSS-II has been provided by the Alfred P. Sloan Foundation, the Participating Institutions, the National Science Foundation, the U.S. Department of Energy, the National Aeronautics and Space Administration, the Japanese Monbukagakusho, the Max Planck Society, and the Higher Education Funding Council for England. The SDSS Web Site is http://www.sdss.org/.

3.3. *Basic Radio Properties*

We have compiled some basic radio data for the 100 X-shaped source candidates: when available, radio flux densities at 365 MHz from the TXS survey (Douglas et al. 1996), 1.4 GHz from the NVSS (Condon et al. 1998), and at 4.9 GHz from the PMN (Griffith et al. 1994, 1995), Green Bank (Becker, White, & Edwards 1991; Gregory & Condon 1991), and Parkes (PKS 5 GHz; Wright & Otrupcek 1990) surveys. These radio data are tabulated in Table A2.

NVSS 1.4 GHz measurements are available for every object (as opposed to the other frequencies) and are probably the most reliable *total* radio flux densities for our candidates. It is the most sensitive, and has the best resolution ($\sim$45″) compared to the other frequency surveys, so is least susceptible to source confusion. The lower resolution VLA configuration used for the survey (compared to the FIRST) means it is better suited to detecting the most extended radio structure.

In six of the largest radio galaxies (J0113+0106, J0147–0851, J0943+2834, J1424+2637, J1501+0752, J1606+0000), it is apparent that they are doubles in the NVSS maps and the integrated fluxes were measured by us. In the case of J1327–0203, we measured the integrated 1.4 GHz flux density from the FIRST map, rather than the NVSS one, so that the 60 mJy contaminating source at the northern edge of the 2' field could be accounted for (Figure A4).

We also inspected the NVSS maps to search for possible larger scale radio structure and to identify potential misidentifications (e.g. our candidate may be part of a field source of another object; see § 5.1). Only two objects, J1049+4422 and J1339–0016, showed hints of diffuse emission that may be associated with our radio source (i.e. they are not due to additional point sources in the field as seen in the higher resolution FIRST images). These possible associations are difficult to determine conclusively because of the mismatch in resolution between the maps (factor of 10 difference between NVSS and FIRST) so this is just mentioned for completeness.

A number of the TXS positions were offset from our determined ones (by $\gtrsim$ 1' in some cases). This is because of the extended (and asymmetric) source structure of many of these radio sources and the limited resolution of the TXS measurements. In the case of the faint source J1456+2542 (36 mJy from NVSS), it is apparent that the TXS measurement was contaminated by other sources visible in the NVSS field so was discarded.

Two-point radio spectral indices relative to 1.4 GHz are also calculated when data at one or both of the other two frequencies were available. No such information was available for 6/100 sources which are among the faintest at 1.4 GHz. Of the remaining, most (90/94) show steep radio spectra ($\alpha \geq 0.5$; $F_\nu \propto \nu^{-\alpha}$) between at least one frequency pair as expected from lobe-dominated radio sources. The remaining four are among the faintest sources, and have single spectral index values as small as $\sim$0.3; we consider these consistent with a steep spectrum considering the possible uncertainties in such low flux density measurements.

4. NOTES ON THE CANDIDATE X-SHAPED RADIO SOURCES

Here, we provide notes on the optical fields and our interpretation of the radio morphologies for each X-shaped radio source candidate in the order presented in Table A2.

(1) J0001–0033: This is a double (east-west) radio source with a clear optical counterpart positioned close to the western lobe. The galaxy is spectroscopically identified by the SDSS with a redshift of 0.25. The more prominent wing is north of the (fainter) eastern lobe in the FIRST image.

(2) J0033–0149: The radio source looks like it could be a winged low-power centrally bright (FR-I) radio galaxy except that we have chosen to associate it with the brightest optically identified source toward the northern edge of the radio source. The bright optical galaxy is at z=0.13 (Jones et al. 2005).

(3) J0036+0048: There is a faint optical object in between the active radio lobes which are approximately oriented east-west. The shorter of the two wings is south of the western lobe.

(4) J0045+0021: Early higher resolution radio maps of this radio source, a.k.a. 4C –00.05 (Downes et al. 1986; Jackson et al. 1999) actually already show the clear X-shaped morphology although it was never noted by these authors. Dunlop et al. (1989) identified a faint optical counterpart (r=21.5 mag.) without a redshift determination – it is too faint to see clearly in the DSS plates. The two most prominent galaxies in the 2' field are probably physically associated with each other, although their relationship to 4C –00.05 is unclear: SDSS J004539.67+002057.6 at z=0.116 (to the west) and SDSS J004543.18+002145.9 at z=0.115 (to the north).

(5) J0049+0059: The optical source is closer to the northern lobe than the southern one and there is diffuse emission in both the east and west directions which may be wings. The optical identification as a z=0.30 galaxy is via the SDSS database. Additionally, there is a prominent z=0.106 galaxy (Rines et al. 2003) $\sim$1' to the northeast (Figure A4).

(6) J0113+0106: This is one of the clearest new examples of an X-shaped source, mainly because of its larger angular extent in comparison to our other candidates. An available lower resolution (NVSS; Condon et al. 1998) map (not shown) shows the faint wing emission more clearly. The optical counterpart (z=0.281; Lacy 2000) is clearly coincident with a faint radio core peaked at 1.4 mJy/bm in the FIRST map. Goto et al. (2002) used SDSS data to identify a cluster of galaxies about 1.5' away directly to the north, but at an estimated z=0.186.

(7) J0115–0000: The optical counterpart to this radio galaxy is a faint source in the DSS red plate at z=0.38 (Lacy 2000). The active radio lobes (north-south) are rather symmetric with clear (although short) wings in the east-west directions.

(8) J0143–0019: This high redshift (z=0.52) radio galaxy was identified by Lacy (2000). From the position he provided [J2000: R.A.=01h43m17s, Dec.=–01d18m59s], we infer that the optical counterpart is the faint smudge in the DSS plate in the eastern lobe (catalogued by the USNO as having a similar red magnitude as provided by Lacy (2000)). If this is indeed the case, then the radio source has quite an asymmetric appearance. The position

we provide is based roughly on where the east and west lobes intersect – a higher resolution 5 GHz image (Reid et al. 1999) shows a bright, compact radio feature near this location. The northern wing is very prominent, but the southern one is not.

(9) J0144–0830: The faint radio source is centrally peaked like an FR-I radio galaxy in the low resolution FIRST image. An optical counterpart near the radio peak is found in the USNO and SDSS catalogues. We imagine the main active radio axis is roughly east-west (more extended) with wings in the orthogonal direction.

(10) J0145–0159: The optical counterpart is the brighter, more centrally located object (relative to the radio source) in the DSS plate. This brighter optical source is identified to be at z=0.126 (Jones et al. 2005) but the fainter (northern) one is unidentified. The (north-south) radio source has clear edges seen to the NW and SE with the wings opposite of them. The b=19 mag object to the south [J2000: R.A.=01h45m19.99s, Dec.=–02d00m24.7s] may have a radio counterpart peaked at 0.4 mJy/bm.

(11) J0147–0851: A faint optical source in the USNO and SDSS catalogs is clearly visible on the DSS red plate and centrally located with respect to the double (NE-SW) radio source. The wing to the south is the more prominent one.

(12) J0211–0920: A pair of optical sources 4″ apart are found near the center of the radio source. We associate the northeastern one of the pair as the optical counterpart since it relates slightly better to the overall radio structure. The western lobe is the brighter one and northern wing is shorter.

(13) J0225–0738: There is a very faint smudge on the DSS plate just to the southern edge of the northern lobe which is catalogued by the SDSS with r=24.3 mag. The more prominent wing is east of the northern lobe and there is some hint of a shorter wing west of the southern lobe.

(14) J0702+5002: The radio source shows very prominent wings to the northeast and southwest. The morphology is suggestive of a FR-I radio galaxy as it is not clearly edge brightened, although this needs confirmation with higher resolution imaging. S. E. Healey (2005, private communication) kindly obtained a spectrum from a 600s exposure at the 2.7m Harlan J. Smith Telescope at the MacDonald Observatory on Oct 30, 2005 and determined a galaxy redshift of 0.0946.

(15) J0725+5835: A faint optical smudge from the USNO catalog is found near the center of the radio galaxy. There is a hint of a small wing to the west. To the east, the possible winged emission is confused with radio emission from a faint optical source with a radio counterpart (∼7 mJy/beam peak in the FIRST image).

(16) J0805+4854: This is one of the smaller angular size radio sources presented in this paper so it is difficult to identify the possible winged emission. The hint of a wing to the southwest is the reason we have included it. There is no clear optical counterpart to the limit of the DSS red plate. There is a very faint r=22.1 ($g-r$=1.1) source SDSS J080543.58+485505.1 toward the northern edge of the radio source which may be the counterpart. Also, a g=16.8 mag SDSS galaxy at z=0.055 appears at the top edge (about 1' to the north) of the 2' wide field of our overlays (Figure A4).

(17) J0813+4347: The active radio lobes appear to run east-west and the more prominent wing is to the north. The optical galaxy is at a modest redshift of z=0.128 as identified by the SDSS.

(18) J0821+2922: This radio galaxy would be very asymmetric if based on the position and identification (z=0.25) given by Willott et al. (2003). Their position is derived from near-infrared imaging (there is indeed a faint optical smudge in the DSS plate at this position with a faint (r=20 mag) counterpart in the SDSS images – we have centered the field in Figure A4 on this position). The radio source is dominated by the southwest lobe in the FIRST image and the southeast wing is very prominent.

(19) J0836+3125: We have centered the field (Figure A4) on a faint optical source appearing in the USNO and SDSS catalogues (r=20 mag). A clear wing appears east of the brighter northern lobe.

(20) J0838+3253: This is one of our less certain identifications as a winged source since it can simply be a slightly distorted FR-I radio galaxy. The peak in the FIRST radio image is offset by about 2″ just to the south of east of the optical galaxy identified to be at z=0.21 by the SDSS.

(21) J0845+4031: The optical counterpart is centrally located in between the two (east-west) active lobes, and the wings are quite prominent. There is a slight twist traced by the radio emission running from the nucleus to the peaks in the lobes. The brighter galaxy about 0.5' to the southwest may just be a field galaxy (identified as a g=18.2 mag galaxy at z=0.096 by the SDSS).

(22) J0846+3956: This is a double (SE-NW) radio source with hints of wings to the east and west. There is no obvious optical counterpart in the DSS image but the SDSS database does give a r=20.8 mag. counterpart.

(23) J0859–0433: This is a very clear example of a winged radio galaxy. The main axis is roughly east-west with a bright hot spot like source at the edge of the western lobe. There is a faint unidentified optical counterpart catalogued in the USNO.

(24) J0914+1715: The FIRST image shows an asymmetric pair of wings with the more pronounced (southern) wing appearing to be associated with the brighter western lobe. A higher resolution 5 GHz image from Haarsma et al. (2005) shows the radio core and the two active lobes characteristic of an FR-II, but the wings are not visible in their image. The optical counterpart is just a faint smudge on the DSS plate and is catalogued by the SDSS at r=20 mag.

(25) J0917+0523: A symmetric double radio source is seen in the FIRST image, with a faint smudge on the DSS plate and catalogued in the SDSS as r=20 mag. A bright optical field source is found at the northern edge of the eastern lobe. The wings are approximately orthogonal to the axis (east-west) of the active lobes.

(26) J0924+4233: This radio source is identified with a z=0.23 galaxy by the SDSS. Wings are quite clearly extended to the north and south of the galaxy. About 1.7' to the southeast (not shown in Figure A4) is a z=0.17 quasar (SDSS J092451.40+423218.9) also recorded by SDSS.

(27) J0941–0143: There are bright symmetric radio lobes aligned to the NE-SW in this z=0.38 galaxy associated with a small cluster (Spinrad et al. 1979). While there is a hint of a short west wing, the eastern one is more prominent.

(28) J0941+2147: The peak in the southern radio lobe is about 5.5 times larger than the northern one. There are two optical sources in the line of sight of the (approximately north-south) radio lobes, toward their edges: a r=19.4 mag one to the north and r=18.2 to the south as catalogued in the USNO but neither appear to be the optical counterparts. Instead, a very faint smudge (r=22.6) is catalogued by the SDSS at the center of the double radio source. A sign of a wing is apparent to the west.

(29) J0943+2834: The double-lobed radio source has a fairly large angular size with a shorter wing to the east associated with the southern lobe. The faint optical source is near a faint central radio peak just discernible in the FIRST image (0.6 mJy/bm).

(30) J1005+1154: The active radio lobes run roughly north-south with a clear optical counterpart in between them identified by SDSS as a z=0.166 galaxy. The galaxy to the southeast about 40″ distant has extended radio emission associated with it.

(31) J1008+0030: This is a radio source associated with the X-ray bright (Brinkmann et al. 1994) cluster Abell 0933 at z=0.098 (Owen et al. 1995). The optical and radio peaks are nearly coincident (Owen et al. 1992) being just 1-2″ offset in our overlay. The FIRST map shows the diffuse emission defining the proposed wings to the SE and NW much better than in a previously published VLA map (Owen et al. 1992).

(32) J1015+5944: This is a higher redshift object at z=0.53, identified as a quasar by SDSS. It is also an X-ray source (Zickgraf et al. 2003). The eastern lobe is about 10 times brighter than the eastern one suggesting that this is the direction of the fore-coming jet. A wing is apparent to the north of the core coincident with an 8.5 mJy/beam peak in the radio. One hopes that the southern wing becomes apparent with deeper observations.

(33) J1040+5056: This radio source looks like a low resolution image of a typical FR-I radio galaxy (e.g., M84; Laing & Bridle 1987). The SDSS identifies the galaxy to be at z=0.154. The brighter (g=18.2), more northerly of the two galaxies to the northwest is identified at z=0.134 by the SDSS (J104017.65+505700.1).

(34) J1043+3131: The radio source is associated with the brightest central galaxy of the triple system (Fanti et al. 1977) at z∼0.036 (Falco et al. 1999) and is an X-ray source (Worrall & Birkinshaw 2000). It has been previously mapped with the VLA (e.g., Fanti et al. 1986; Parma et al. 1986) showing hot spots aligned at PA∼162°. The extended emission perpendicular to this axis can then be interpreted as wings.

(35) J1049+4422: The faint optical counterpart is closer to the northwest lobe, which shows the apparent wing to the south. This galaxy is only about 1.5 arcmin from the galaxy cluster Abell 1101 at z=0.23 which is to the southeast (Struble & Rood 1999).

(36) J1054+5521: There is no clear optical counterpart to the radio source in the DSS plates thus the position is based on where we expect the optical counterpart to be relative to the radio structure (in between the east-west lobes). Some faint optical smudges appear toward the edges of the eastern lobe.

(37) J1055–0707: The radio source is quite symmetric looking centered about the bright optical counterpart. The DSS image has a streak across it with unknown origin. The wings are quite clear poking out the sides of the axis of the main (NE-SW) lobes.

(38) J1102+0250: The SDSS cataloged a faint (r=22.3 mag) counterpart near the central radio peak (12 mJy/beam); this is not obvious in the DSS plates. The could simply be a normal double-lobed radio source but the diffuse structure to the southwest of the southeast lobe is suggestive of winged emission.

(39) J1111+4050: The radio source appears to be associated with the z=0.074 galaxy MCG+07-23-030 in the X-ray bright (Ledlow et al. 2003) cluster Abell 1190 (Slinglend et al. 1998). If this is the case, this is unlikely to be an X-shaped radio source because of the implied asymmetry; our original interpretation would have been that the active lobes are marked by the roughly east-west peaks with a very prominent wing to the south.

(40) J1114+2632: A roughly centrally peaked radio source (64 mJy/beam) in the FIRST map with a faint optical counterpart of 22.0 mag in the APM blue plate but without a red counterpart (>20.0 mag) in the limit of the APM plate (Snellen et al. 2002). These are consistent with the SDSS detections (e.g. r=21.0 mag). The low frequency spectrum (between 0.365 and 1.4 GHz) is steep α=0.77, then flattens to 5 GHz, suggesting that an optically thick component emerges at the higher frequencies.

(41) J1120+4354: A fairly symmetric (NE-SW) double-lobed radio source with small wings about a faint optical source in the red DSS image (r=20.4 mag in the SDSS). The radio field source to the northwest is peaked at 4.6 mJy/bm.

(42) J1128+1919: The bright r=16.1 mag optical source catalogued by the USNO matching the position of the peak in the southern radio lobe (about 13″ from the center of the radio source) is probably a field source. Optical emission from the center of the radio source is not visible in the DSS image so we base the position on the radio structure. Curiously, the SDSS catalogs an optical source very near this approximated position (SDSS J112838.05+191956.7), however, there is hardly anything visible in their images and the photometry does not appear robust (e.g. r=24.2 mag, with $g-r$=–1.6) – this may be the counterpart but should be confirmed with deeper imaging. The shorter proposed wing is east of northern lobe.

(43) J1135–0737: A faint optical counterpart to this clear X-shaped radio source (main lobes are north-south) was recorded in the USNO catalogue. A more prominent optical source (b_J=17.88 mag) can be seen in the field overlapping with the outer edge of the southwest wing.

(44) J1140+1057: The SDSS identifies this as a nearby (z=0.081) radio galaxy. The wing to the south of the eastern lobe is more prominent than the one north of the western lobe. A bright optical field source is seen off the edge of the eastern lobe.

(45) J1200+6105: A wing to the south is clear but its northern counterpart is not apparent in this double-lobed (approximately east-west) radio source. The optical counterpart is near the center of the radio source as expected.

(46) J1201–0703: The radio source consists of a northern pointing lobe (close to the optical counterpart) and an extensive southeastern lobe. Extended emission, perhaps from a wing, is seen to stretch from the northeastern part of the northern lobe. Possible wing emission to the south seems to be associated with a b=19.5 mag source found in the APM catalog [J2000: R.A.=12h01m26.93s, Dec.=–07d03m44.4s] with a radio peak of 13 mJy/bm.

(47) J1202+4915: There is no clear optical counterpart in the DSS plates to this faint radio galaxy but one was found (r=21 mag) in the SDSS database. The FIRST image suggests the appearance of a pair of faint east-west wings.

(48) J1206+3812: This radio source was identified as an r=18 mag quasar at high redshift (z=0.838) on the basis of MgII and OII lines by Vigotti et al. (1990). This is confirmed by the SDSS. If the X-shaped morphology can be confirmed, this is by far the highest redshift X-shaped source known. It shows a bright double-lobed radio morphology which is quite symmetric.

(49) J1207+3352: This B2 radio galaxy has been studied by Parma et al. (1986) with the VLA and Capetti et al. (2000) with HST. It is identified with a z=0.0788 galaxy in Fanti et al. (1987). The optical and radio core emissions peak very closely. The FIRST image shows similar structure to what is seen in Parma et al. (1986).

(50) J1210–0341: The radio lobes run in the NW-SE direction with orthogonal low surface brightness wings quite apparent even in the limited resolution FIRST image. The optical source near center is identified with a z=0.26 galaxy (Machalski & Condon 1999).

(51) J1210+1121: The z=0.2 (SDSS) galaxy is just offset from the southwest peak of the radio source giving this a very lop-sided appearance. The proposed western wing is very extended at over 1 arcmin in length.

(52) J1211+4539: A faint optical counterpart (r=22 mag) found in the SDSS database. This is too faint to be readily visible in the DSS plates. There is a hint of wings for this symmetric radio double (NW-SE active lobes), although they not very extended in the FIRST image.

(53) J1218+1955: Symmetric radio source (NE-SW) with a faint optical counterpart near its center. The wings are short (projected) relative to the active lobes.

(54) J1227–0742: The nearest plausible optical counterpart is the nearby (z=0.029; Fairall et al. 1992) b=15.0 mag galaxy MCG -01-32-011 about 0.2' offset from the center of the radio source; however, if this is the case, this would make the radio source quite asymmetric and unusual looking. We rather favor that the optical counterpart could be near the center of the radio source, in between the two active lobes (NW-SE), and is hidden by the galaxy light from MCG -01-32-011. In this case, the two extended diffuse east-west emission would be interpreted as wings.

(55) J1227+2155: A faint optical source near the center of the radio source was found in the USNO and SDSS catalogues. There appears to be two active lobes just off the east-west axis, with more extended lower surface brightness wings of radio emission north and south of the optical source.

(56) J1228+2642: A pair of optical sources appear overlapping the radio structure; we associate the radio source with the brighter of the two (more northern) as it is more centrally located relative to the radio emission. We imagine that the radio lobes run north-south; the more extended western wing would be associated with the southern lobe.

(57) J1232–0717: A faint optical counterpart was identified in the USNO catalog. The radio source is double-lobed in the east-west direction with the more extended proposed wing to the south.

(58) J1247+4646: A faint optical counterpart (SDSS r=22 mag) to this radio source. There are hints of wings to the NE and SW.

(59) J1253+3435: The estimated redshift of 0.034 (Brand et al. 2005) may be underestimated – it implies a lower radio luminosity than would be expected from its FR-II morphology ($L_{1.4\mathrm{GHz}} = 10^{24}$ W/Hz). The radio source has been mapped at higher resolution than the FIRST image presented here by Machalski & Condon (1983). Their map shows the a more compact hot spot in the northeast lobe but failed to detect the diffuse emission shown in the FIRST map.

(60) J1258+3227: The r=17 mag (SDSS) source close to the northwest lobe appears to be the parent object of this radio galaxy. The wing to the south of this lobe is obvious but no wing is apparent on the opposite lobe.

(61) J1309–0012: The optical counterpart is centered between the east-west radio lobes. It is much more apparent in the R-band image of Best et al. (1999). They identify this as a radio galaxy at z=0.42. The wing to the south of the western lobe is seen also in their 5 GHz image of similar resolution to the FIRST image; there is a suggestion of a short wing north of the eastern lobe in the FIRST image. The optical sources just overlapping with the eastern radio lobe is suggested to be part of a cluster, SDSS CE J197.463455-00.213781 at an estimated z=0.367 (Goto et al. 2002).

(62) J1310+5458: The central radio component in the low resolution FIRST image is peaked (23 mJy/beam) very near the optical counterpart. The active lobes form an east-west axis with the core component, and the wing-like extensions are orthogonal to this.

(63) J1316+2427: A faint optical counterpart is found in the USNO and SDSS catalogs at the center of this faint double (approximately east-west) radio source. One can imagine a pair of short faint wings to the north and south.

(64) J1327–0203: The radio source is identified with an SDSS galaxy at z=0.18. The north-south wings are quite prominent although need higher resolution observations to improve the detailing of the overall morphology.

(65) J1330–0206: We associate the radio source with the brightest (g=16.6; z=0.09 from SDSS) member of the southern sub-cluster of Abell 1750 (Beers et al. 1991). This particular galaxy is near the center of the double-lobed (approximately east-west) structure. The galaxy at the

southern edge of the eastern lobe is a fainter (g=19.2 mag) cluster member.

(66) J1339–0016: Downes et al. (1986) pointed out that the z=0.145 (SDSS) galaxy near the southern peak of this powerful extended radio source (a.k.a. PKS 1137–000) is probably the optical counterpart, rather than the z=1.818 quasar (Croom et al. 2001) that is the faint optical smudge at the eastern edge of a northern lobe component [J2000: R.A.=13h39m33.9s, Dec.=–00d16m13s]. The optical galaxy is in between two radio peaks toward the southern edge of the radio source. The galaxy is in the field of the SDSS galaxy cluster SDSS CE J204.901352-00.280581 at and estimated z=0.16 (Goto et al. 2002). The western wing associated with the northern lobe is quite prominent while the eastern wing of the southern component takes a dramatic southerly bend after extending to the east/northeast.

(67) J1342+2547: The optical counterpart of this roughly north-south radio source is closer to the fainter southern lobe. The wings are quite clearly extended in roughly the east-west directions.

(68) J1345+5233: We have found a faint smudge in the DSS red plate very near the peak of this faint centrally-peaked radio source. This source is catalogued in the SDSS database. In the low resolution FIRST image, there appears to be four radio extensions directed outward from the optical source. The east-west axis is more extended.

(69) J1348+4411: The radio lobes run north-south and are not quite symmetric with respect to the optical counterpart. The wings are pretty clear – the western wing off the southern lobe runs out to $\sim$30″ marked by the single contour (Figure A4).

(70) J1351+5559: This is a distorted radio source with several galaxies in the near field determined to be at z$\simeq$0.07. However, there is no redshift determination for the bright galaxy we have associated with the central radio source. One can imagine the radio lobes oriented roughly east-west and that there are wings to the south-north with an extended spur of emission in the southern direction. The two neighboring galaxies to the north are probably physically associated: SDSS J135142.56+555957.7 (g=17.8; z=0.06786±0.00008) and the slightly brighter more northerly SDSS J135142.13+560004.5 (g=17.3; z=0.07036±0.00019). Another physically associated galaxy is about 2' further north (not shown), SDSS J135140.26+560125.1 (g=18.0; z=0.06789±0.00015).

(71) J1353+0724: There is a distracting gradient across the DSS red image; otherwise, the optical counterpart is clearly centered in between the radio lobes. A wing appears to the north, associated with the fainter western lobe.

(72) J1406–0154: There is a faint optical smudge in the DSS red plate (SDSS r=21 mag) near where the two radio lobes cross. In the FIRST image, there is emission suggestive of a wing to the south of the western lobe and a shorter one north of the eastern lobe.

(73) J1406+0657: There are clear extended wings in the NW-SE direction roughly orthogonal to the axis of a double-lobed radio structure. The central radio peak is coincident with an optical source in the USNO and SDSS catalogues.

(74) J1408+0225: The radio structure is barely resolved in the FIRST image but is suggestive of having lobes running east-west and that there is a more prominent wing to the south. The optical counterpart, found in the USNO and SDSS catalogs, is coincident with the FIRST radio image peak of 40.6 mJy/beam.

(75) J1411+0907: A faint optical source in the USNO and SDSS catalogues appears in between the two radio lobes. An extended wing to the southwest of the southern radio lobe is obvious but one associated with the northern lobe is not apparent in the FIRST image.

(76) J1424+2637: This nearby B2 radio galaxy is identified with MCG +05-34-033 (z=0.037; Miller et al. 2002) and has been extensively studied. It has been imaged in the radio (e.g., de Ruiter et al. 1986), with HST (Capetti et al. 2000), and is an X-ray source (Canosa et al. 1999). The wing north of the eastern lobe is shorter.

(77) J1430+5217: The optical counterpart is coincident with the central peak (26 mJy/beam) in the FIRST image. This object is identified as a quasar at z=0.367 in the SDSS spectrum. The southwest wing is slightly more extended than the northeastern one.

(78) J1433+0037: A faint optical smudge in the DSS plate and found in the SDSS catalog is coincident with a radio peak (4 mJy/beam) near the center of this radio galaxy. A wing is quite clear to the east of the northern lobe, however, the "wing" from the southern lobe runs to the south, not west as would have been expected.

(79) J1434+5906: We find a faint smudge in the DSS red plate centered between the two lobes oriented in the NE-SW direction. The southeast wing is much more prominent. In the field, we see SDSS J143406.28+590704.5, a g=15.4 mag galaxy at z=0.040 (a faint radio counterpart peaked at 0.6 mJy/beam in the FIRST image), prominently 30″ away north of east of the radio galaxy.

(80) J1437+0834: A faint optical counterpart was catalogued by the USNO and SDSS near the center of double (east-west) radio source. The more prominent wing is north of the western lobe.

(81) J1444+4147: The optical counterpart is a z=0.188 galaxy from the SDSS and is centered on the radio source. There is a (SDSS z=0.255) galaxy in the field only 0.4 arcmin away overlapping the eastern lobe. We suggest the low surface brightness emissions to the north and south are wings.

(82) J1454+2732: There is no obvious optical counterpart to this (north-south) radio source in the DSS image shown in Figure A4, but a r=20 mag object is catalogued in the SDSS. The southern lobe is extended and the wing east of the northern lobe is apparent.

(83) J1455+3237: The optical field is a bit busy with several field sources appearing in the DSS image. The optical source we have chosen as the counterpart is a bright (r=16 mag) object at a z=0.084 (SDSS) and is closest to the center of the radio source. The main axis is roughly east-west and there is an extension to the north that is suggestive of winged emission.

(84) J1456+2542: A very faint r=20.6 mag counterpart in the SDSS catalog is centered on the faint radio source.

We imagine the main lobes to be oriented north-south with the more prominent wing east of the northern lobe.

(85) J1459+2903: The mainly north-south radio source shows a hint of additional extended emission east of the north lobe rather than a sharp edge characteristic of X-shaped sources. The proposed wings are east and west of the galaxy. This was previously studied with the VLA and HST by Fanti and collaborators (e.g., Fanti et al. 1987; Capetti et al. 2000) as part of their studies of B2 radio galaxies and could very well be a normal radio galaxy. The radio peak (22 mJy/beam) in the FIRST image is coincident with the optical source identified with a z=0.146 galaxy (González-Serrano & Carballo 2000).

(86) J1501+0752: A faint smudge appears near the center of the double-lobed radio source in the DSS plate. The SDSS catalog lists this smudge as a r∼21 mag object and we have centered the field on this source. There is a clear wing north of the northern lobe but the wing associated with the southern lobe is not as obvious.

(87) J1515–0532: The radio source is fairly large in the sky (∼1.5 arcmin in extent) and straddles a very faint smudge in the DSS plates – we have chosen to center the field on this smudge catalogued in the APM. The wings are short in projection (west of the north lobe and east of south lobe) if they are indeed winged emission.

(88) J1522+4527: There are two z=0.277 SDSS galaxies overlapping the radio structure but neither are clearly the nucleus of the radio source if this is a double-lobed radio galaxy (both optical sources are near the outer edge of the radio lobes). The more centrally located (relative to the radio source) galaxy (SDSS J152212.52+452804.7; g=19.2) is only 0.2 arcmin to the north of the gap between the radio double; the other is 0.9 arcmin away (SDSS J152210.97+452708.7; g=20.4). There are hints of low surface-brightness emission around the source, especially to the east, which may be wings.

(89) J1537+2648: There is a clear optical counterpart coincident with a central radio peak in between the two (NW-SE) radio lobes. A very prominent wing associated with the northern lobe stretches to the northeast but the one associated with the southern one is not obvious in the FIRST image.

(90) J1600+2058: This is a good example of an X-shaped radio source with a morphology suggestive of a low-power FR-I radio galaxy. The optical counterpart has not yet been spectroscopically identified.

(91) J1603+5242: The optical counterpart is aligned with an obvious radio core in an edge-brightened (NW-SE) radio source. The shorter wing is west of the southern lobe while the one associated with the northern lobe is quite obvious.

(92) J1606+0000: The radio source has been identified with a nearby, z=0.059 galaxy (Best et al. 1999) whose ellipticity is quite obvious in the DSS image. A high resolution 5 GHz VLA map shows what appears to be a one-sided jet directed to east although there is a mismatch between the brightest radio component and the center of the optical galaxy in the overlay shown in Best et al. (1999). The very extended radio wings to the north and south revealed in the FIRST map do not appear in their high resolution map.

(93) J1606+4517: There is faint optical counterpart (r=20.5 mag) in the SDSS catalog centered on north-south double radio source. The more prominent wing we propose is east of the northern lobe.

(94) J1614+2817: The radio lobes are aligned roughly east-west with a pair of prominent wings in the orthogonal direction. The optical identification comes from Miller & Owen (2001) who found it to be nearby galaxy at z=0.107.

(95) J1625+2705: This object is identified as a fairly distant (z=0.526) quasar in the SDSS and is a known X-ray source (Wolter & Celotti 2001). The radio morphology is centrally peaked in the FIRST image with extended emission to the east/northeast suggestive of a wing.

(96) J1653+3115: Two adjacent (NE-SW) very faint optical smudges are seen in the DSS plate near the center of the radio source – the central radio peak (40 mJy/beam) is offset by ∼2″ from the closer of the two (the SW one). We imagine the main active lobes running in the NW-SE direction.

(97) J1655+4551: A faint uncatalogued optical smudge is found in the DSS red plate toward the northeast part of the radio source. We suggest the presence of at least one wing toward the west if the main lobes are in the NW-SE direction.

(98) J1656+3952: An optical counterpart was found in the DSS image coincident with a central radio component (11.5 mJy/beam peak in the FIRST image) between the roughly east-west lobes. One wing is seen to the south of the eastern lobe but the wing in the opposite direction is not as obvious in the FIRST image.

(99) J2226+0125: The center of the radio source (i.e. the gap between the two active, north-south lobes in the FIRST map) is approximately midway (∼7″) between two possible optical counterparts. Based on its position relative to the radio structure, the northern b_J=19.9 mag galaxy [J2000: R.A.=22h26m45.44s, Dec.=+01d25m17.5s] is our best guess but this is not definitive. For reference, the galaxy overlapping the southern lobe is a b_J=19.5 mag galaxy [J2000: R.A.=22h26m45.87s, Dec.=+01d25m05.8s], both from the APM catalog. Both are members of the Zwicky cluster ZwCl 2224.2+0109 (Zwicky et al. 1965). Two wings are quite obvious with the one associated with the southern lobe protruding more toward the outer edge of the lobe rather than the side.

(100) J2359–1041: We identify the r=19 mag (SDSS) optical source near the central peak of the mainly east-west radio source with the host. Two brighter optical field sources overlap with the radio source: one just ∼5″ north of the optical counterpart and the other in the western lobe, 17″ away. The proposed wings are north of the western lobe and south of the eastern lobe.

5. DISCUSSION

We address four issues pertinent to the search and study of X-shaped radio sources. First, we gauge the success of our method by taking a census of known examples from the literature to determine the efficiency in which they are recovered by our method (§ 5.1). Some basic properties of the candidates are compared to those of the known

examples (§ 5.2). We then explore source orientation, projection, and evolution effects on the observed morphology in § 5.3, and briefly discuss the possible misidentifications in our search (§ 5.4).

5.1. *Census and Success of our Method in Identifying Known Examples*

Of the 19 known winged and X-shaped sources listed in Table A1 (§ 2), 11 have FIRST coverage in the current data release and the efficiency in which they are recovered allow us to gauge the limitations of our search process. The results can be summarized as follows (see Table A1, column 10):

- Nine objects contain at least one component in the radio source satisfying our selection criteria (>5 mJy/bm peak and FWHM>5″; § 3.1). Five are readily identifiable as X-shaped sources in the FIRST maps (4C+01.30 was actually originally identified as an X-shaped source from its FIRST image; Wang et al. 2003). The remaining four, the largest among the known examples, were "missed" because of their large angular sizes. Although their double lobed nature are evident in some of the FIRST maps, their low surface brightness wing emission were resolved out.
- In the two remaining cases, our peak flux and component size thresholds are set too high and we would not have inspected their FIRST field images. The angular size of the double-lobed structure in J1357+4807 is small and none of its diffuse winged emission was distinguishable in the FIRST map. In J2157+0037, its X-shaped nature is quite evident in the FIRST map (we identified it in a printed version in Zakamska et al. 2004). However, although its eastern lobe is very bright (50.8 mJy/bm peak), its deconvolved size of 4.85″×3.24″ is just under our threshold of 5″.

In one of the missed cases (4C+48.29), the FIRST image field containing its southern lobe/hot spot complex was initially selected for further scrutinization based on its double structure and surrounding diffuse emission (Figure A3). It was subsequently removed from our list because of its association with 4C+48.29 in the NVSS map.

All 19 objects have NVSS coverage, and as realized in the 4C+48.29 case, many of these are distinguishable as X-shaped sources in the ∼45″ resolution maps while they are too large to be distinguished in the FIRST maps (see above). Conversely, many of the smaller angular size ones identifiable in the FIRST images (e.g., 3C 63, 4C+01.30, 4C+04.40) are unresolved in the NVSS maps. This gives a complementary approach of the two surveys for this work. However, short wings in large angular size sources (e.g. 3C 192, 3C 379.1) are not distinguishable in the low resolution NVSS maps, while the FIRST images resolve out the diffuse emission (like in 3C 192). The main limiting factor in any NVSS search is that it is sensitive only to bright, prominently winged large angular size sources and the majority of these have probably already been identified. See column 11 in Table A1 for a summary of the FIRST and NVSS search results of the known sources.

5.2. *Radio Luminosity*

Figure A2 shows the 1.4 GHz radio luminosity–redshift ($L-z$) distribution of the spectroscopically identified (36) candidate winged and X-shaped radio sources along with the (18) examples we compiled from the literature; the quasars from both samples are marked as such. We see that the flux limit of our FIRST-based sample is effectively ∼100 mJy, while the majority of the widely known examples (from the lists of Leahy & Parma 1992; Rottmann 2001; Capetti et al. 2002) have 1.4 GHz flux densities $\gtrsim 1$ Jy. This means we are identifying X-shaped radio sources with systematically lower radio luminosities for a given redshift (by about 1 order of magnitude) than those from previous catalogs. In fact, the four most recently identified X-shaped sources in the literature have flux densities comparable to our FIRST candidates (J1130+0058 and J2157+0037 were actually identified in FIRST radio maps).

The lower flux threshold makes it possible to identify more distant, and intrinsically lower luminosity (at a given redshift) radio sources as X-shaped candidates. Simply by inspecting published maps, we extended the redshift limit of known X-sources from z ∼0.3 to ∼0.4 with J1357+4807 (Lehár et al. 2001) and J2157+0037 (Zakamska et al. 2004). We can extend our census even further if we can confirm the morphologies in a number of our candidates (four radio galaxies, J0115–0000, J0143–0118, J0941–0143, and J1309–0012 at z=0.38 to 0.52, and four quasars from z=0.37 to 0.8).

In such flux-limited samples, the lowest luminosity objects (like the FR-I's) are naturally deselected out. This makes it important to confirm if some of the less-luminous, more centrally peaked candidates (e.g. J0144–0830, J1345+5233, J1600+2058) do indeed have FR-I radio morphologies (like e.g. 3C 315, Alexander & Leahy 1987). Unfortunately, these are not yet optically classified and are among the faintest and smaller angular size radio sources in our compilation. Consequently, from Figure A2, we see that to probe the high redshift counterparts of the lower luminosity z<0.3 population (∼10^{24-26} W/Hz), we must go fainter than $\lesssim$ 100 mJy at 1.4 GHz.

For the 16 X-shaped radio *galaxies* with spectroscopic identifications comprising the "literature" sample (Table A1), we find an average 1.4 GHz luminosity of log L [W/Hz] = 25.85 (1σ standard deviation = 0.64; median=25.95). As X-shaped radio sources are known to have radio luminosities close to the Fanaroff & Riley type-I/II division, this was expected[7]. Including the 32 candidates identified radio-galaxies from our study brings the average luminosity even closer to the FR-divide (<log L> [W/Hz] =25.49 with 1σ =0.71; median =25.31), although the large spread does not make this change statistically significant. Including the quasars, where a portion of the emission may be affected by Doppler beaming

[7] More precisely, they are found preferentially in low-luminosity FR-II's (Leahy & Parma 1992; Dennett-Thorpe et al. 2002). The original Fanaroff & Riley (1974) division of 6.3×10^{25} W/Hz/h^2 at 178 MHz translates to ∼few $\times10^{25}$ W/Hz at 1.4 GHz for our adopted cosmology and typical spectral index values around unity.

(<log L>=26.3 W/Hz for the six examples), has little affect on the values quoted as there are but a few of these. The connection to the Fanaroff-Riley luminosity division is unclear although it is tempting to associate this with their transitory appearances – are these the long sought transition objects between FR-I's and FR-II's? However, any definitive statements would be premature as for instance, one is reminded that not all the candidates are yet confirmed X-shaped radio sources.

If one were however to pursue this association further, we must explain the large range of observed luminosities of the X-shaped sources from $\sim 10^{24-27}$ W/Hz. This may find a natural explanation in the fact that the radio luminosity dividing the Fanaroff-Riley type-I from type-II morphology sources is known to be dependent on the parent host galaxy magnitude over a comparable radio luminosity range (e.g., Ledlow & Owen 1996)[8]. Further radio imaging of our candidates and a dedicated host-galaxy imaging program can determine the proper placement of X-shaped radio sources in the Owen-Ledlow plane, which may serve as a useful diagnostic of the physical origin of these peculiar objects.

5.3. *Source Orientation, Projection and Evolution Effects on the Appearance of X-shaped Radio Sources*

Observationally, one expects winged/X-shaped sources to be most apparent when *both* the wings and active lobes are projected close to the plane of the sky. It is then no surprise that so far, the majority of them have tended toward galaxies with narrow-line systems (Wang et al. 2003). In unified schemes (Orr & Browne 1982; Barthel 1989), these are the radio galaxies with active lobes projected near the plane of the sky. We must then consider the effects of projection and source evolution on their appearance for any attempt at a complete census of this class of objects. This motivated us to include candidates with shorter wings (i.e., wing to lobe length ratios <0.8 like 3C 192 and 3C379.1; see § 5.1), more amorphous looking ones, and sources with smaller angular sizes in compiling our candidate list.

Four of the spectroscopically identified X-shaped radio source candidates are identified as (higher redshift; z=0.4–0.8) quasars, adding to the two known examples (at lower-redshifts; Table A1). The relatively few but increasing number of X-shaped quasars may be because their active lobes are aligned closer to our line of sight and higher dynamic range is required to detect the (unbeamed) low-surface brightness wings. Additionally, the number density of quasars peak at $z \sim$1–2 (e.g., Boyle et al. 2000), so naively, we expect more X-shaped quasars to be identified as we push to high-redshifts. As an extreme case, Marecki et al. (2006) has recently pointed out that the z=2.065 quasar 0229+132 (Murphy et al. 1993) may be one of the most extreme case of an aligned X-shaped radio source with its large core-dominance. A significant population of X-shaped radio quasars may have hitherto gone unnoticed.

Source distance will also affect the appearance of an X-shaped radio source. For a given surface brightness (or constant wing luminosity), the natural $(1+z)^4$ dimming of radiation makes it more difficult to detect winged sources at high redshift. This may be why the two lower-redshift (z<0.3) X-shaped radio quasars from the literature (Wang et al. 2003; Landt et al. 2006) have more prominent wings than our higher redshift candidates. In a flux-limited sample, the higher-redshift sources tend toward having higher luminosities (e.g., our quasar candidates are an order of magnitude more luminous than the two lower-redshift ones from the literature); this and cosmological dimming may explain the small number of high redshift X-shaped radio galaxies and quasars identified so far (our high-z candidates need improved radio imaging to confirm their X-shape).

As alluded to earlier, the extent of the wings can simply be foreshortened by projection. In the active lobes, asymmetry/sidedness of the opposite jets serve as a proxy of source orientation (e.g., Orr & Browne 1982; Barthel 1989). As an analogue, the pronounced asymmetry in the relative prominence between the two wings in some objects may indicate that the wings (in the realignment scenario, this is the original source axis) are aligned close to our line of sight. Depolarization asymmetry in the wings could for example, then determine the importance of projection in the wings – this has been used as a proxy of source orientation in the lobes of classical doubles (Garrington et al. 1988; Laing 1988).

If we can disentangle projection from intrinsic (i.e. source evolution) effects, the extent of the wings may indicate the evolutionary stage of the radio source. In a hydrodynamic origin, long wings means maximal backflow activity but short wings may either indicate the initial or terminal stages of source activity. In the realignment scenario, the maximal extent and surface brightness of the wings occurs shortly after realignment and decreases thereafter. Radio spectral mapping of the lobes and wings (spectral index and break frequency) can thus "date" the radio source (Klein et al. 1995; Dennett-Thorpe et al. 2002) to differentiate between these possibilities.

In the evolution scenario, we should be able to see a continuum of wing to lobe ratios with values so large as to create wing-dominated objects (at the other extreme are lobe-dominated objects which are the classical doubles). These could masquerades as CSS or GPS sources (O'Dea 1998). As an extreme example, Maness et al. (2004) recently found such a GPS source with a large scale structure and a inner double source with flat radio spectra (they associate these with a pair of AGN). Another possibility is that of the "relaxed doubles" which have radio lobes appearing to be fading; two classic examples (Hercules A and 3C 310) have been found to have parsec-scale structures misaligned with the large-scale lobes (Gizani & Garrett 2002). Finally, the borderline FR-I/II radio galaxy 3C 293 (z=0.0452) was identified early on as a possible progenitor of the X-shaped sources (Bridle et al. 1981; Dennett-Thorpe et al. 2002). Its inner $\sim$2 kpc (0.88 kpc per arcsec) double-sided source straddles a flat spectrum radio core which is coincident with the optical nucleus; this is misaligned by $\sim 30^\circ$ from the $\sim$200 kpc double larger structure. Dennett-Thorpe et al. (2002) noted that 3C 293 shows the "shortest ratio of active lobe length to wing length is the only one which shows clear evidence for a recent merger" (cf. Floyd et al. 2006).

5.4. *Possible Misidentifications*

[8] Converting to our adopted cosmology, the corresponding luminosities are $\sim$15–30% larger for the range of redshifts considered.

With more sensitive, higher resolution radio imaging of these candidates, many of them will turn out to be bona-fide X-shaped radio sources. The remaining will probably turn out to be simply winged sources, and a few are likely unrelated to the X-shaped phenomenon.

In particular, some of the objects may be "bent-doubles," which have been targeted previously in a similar search through the FIRST database (Blanton et al. 2001). Two (J0033–0149, J1111+4050) resemble narrow-angle tail (NAT) radio sources (e.g., O' Dea & Owen 1985). As other examples, the referee has cited "J0813+4347, J1330-206 as plausible NATs and J0838+3253, J1339-0016 as possible WATs" (wide-angle tailed), and the author concurs. Finally, J0145–0159 and J1040+5056 may turn out to be entirely normal FRI radio galaxies (§ 4), while J1043+3131 and J1351+5559 appear quite distorted in the low resolution maps. Such sources will probably contaminate the final winged and X-shaped source samples at the ∼10–20% level. This makes new radio observations necessary to confirm or not the present morphological identifications.

6. SUMMARY AND FUTURE WORK

A satisfactory explanation for the origin of the wings that give the X-shaped radio galaxies their characteristic morphologies remains elusive. This is mainly because of the small number studied in detail, and the small total number of known examples available for systematic studies. This was the motivation for this FIRST-based search for new examples. Candidates were selected by visual inspection of radio sources fields containing resolved structure and imaged with sufficient fidelity to be able to identify the winged structures. This paper presents an initial sample of 100 candidates drawn from a subset (∼1/5th of a total ∼8,000 sources) of the currently data release matching our criteria.

Of the 100 candidates, we found optical identifications for 94 of the radio sources. Almost 40% of these have spectroscopic identifications available from the literature, many from the SDSS database. In the radio luminosity-redshift plane, it is clear that we are systematically probing an order of magnitude lower radio luminosities than previous samples. This allows us to identify candidates at higher redshifts and a handful of objects with morphologies characteristic of low-luminosity FR-I radio galaxies. If confirmed, such objects challenge current models for the formation/origin of X-shaped radio sources – powerful jet driven cocoons which are characteristic of FRIIs are required to form the new active lobes in the merger scenario (Gopal-Krishna et al. 2003) and to drive the backflow in the hydrodynamic picture of Capetti et al. (2002).

We find an average radio luminosity of the combined sample from the literature and our candidates to be close to the classical Fanaroff-Riley division, albeit with a large spread. It may be a useful to project these data onto the Owen-Ledlow (i.e. host galaxy magnitude vs. radio luminosity) plane to explore the relationship of these objects with the Fanaroff-Riley division.

This is only the first step in a systematic study of these objects. Higher resolution imaging with the VLA are in progress and will detail the candidates' morphologies to confirm or not their X-shaped nature. Follow-up multi-frequency imaging of bona-fide X-shaped sources will be able to reveal spectral differences between the wings and lobes and any spectral structure to set upper limits on the particle ages in the wings, thus on the source lifetime (e.g., Klein et al. 1995; Dennett-Thorpe et al. 2002). Observations can also detail the varying prominence of the 'Z' in the morphologies, which have been taken as a sign of an ongoing merger (Gopal-Krishna et al. 2003; Zier 2005). This scenario may lead to observable displacements in their emission lines (Begelman et al. 1980) and between the radio core and optical nucleus (Madau & Quataert 2004) – an optical spectroscopy program (in progress) and sensitive VLBI imaging of the X-shaped radio sources with prominent radio cores are necessary to test these interesting possibilities.

An important issue in the formation of X-shaped radio sources is in their environments. This can be constrained with X-ray data (Worrall et al. 1995; Kraft et al. 2005), an examination of their optical fields (are these preferentially in groups or clusters?), and radio polarization observations (Dennett-Thorpe et al. 2002). These can be compared to the properties of classical radio galaxies (e.g., Zirbel 1997). Also, a determination of their host galaxy properties may provide additional clues as to their origin (e.g., Ulrich & Roennback 1996; Capetti et al. 2000). This work lays the groundwork to produce an extensive sample of X-shaped sources in order to carry out the follow-up work necessary to test the differing possibilities.

Acknowledgments

The inspiration to mine the FIRST database came after a colloquium talk by David Helfand (in April 2005) at the MIT Kavli Institute (MKI), where the author's fellowship was initially hosted. He is grateful to the MKI and his current host, the KIPAC at Stanford for their hospitality. Stephen Healey and Hermine Landt provided valuable assistance and advice in the optical identifications. Dan Harris, Christian Zier, and the anonymous referee gave very useful comments which improved the manuscript.

APPENDIX

NOTES ON NEW X-SHAPED RADIO SOURCES FROM THE LITERATURE

We provide brief descriptions of X-shaped radio sources not included in the earlier compilations of Leahy & Parma (1992, see Merritt & Ekers (2002)), Rottmann (2001), and Capetti et al. (2002). See Table A1 for the complete list. Figure A5 shows the radio/optical overlays for the 3/5 sources below with the X-shaped structures apparent in the FIRST images.

J1130+0058: This X-shaped radio source (4C+01.30) was discovered in a FIRST map (Figure A5), and studied in detail by Wang et al. (2003). It is the first case of an X-source with a quasar nucleus, at a moderate redshift of 0.132.

J1206+0406: The X-shaped nature of J1206+0406 was uncovered in a low-frequency (320 MHz) VLA map by Junor et al. (2000) and we confirmed the morphology in the FIRST map (Figure A5). The radio structure has an asymmetric appearance showing a one-sided jet to the southwest and a diffuse lobe opposite of the core. The northwestern wing is much more prominent than the one to the southeast. No redshift is available for J1206+0406 but we found a r=20.5 mag. optical counterpart in the SDSS (J120620.12+040610.7, $g-r$=0.95).

J1357+4807: We chanced upon a published 1.4 GHz VLA map of J1357+4807 (Lehár et al. 2001, Figure 2 therein) which showed faint wings on the NE-SW axis. They associate it with a R=19.7 mag object from the APM; we confirm the identification as SDSS J135730.6+480741.7 (r=20.1 mag.; $g-r$=0.9). We obtained a spectrum with the Hobby-Eberly Telescope and found this to be a z=0.383 narrow-line radio galaxy (C. C. Cheung & S. E. Healey 2006, unpublished).

J2157+0037: We also chanced upon a (FIRST) map of this candidate type-II AGN in Zakamska et al. (2004) which shows the X-shape very clearly (Figure A5). The optical counterpart (SDSS J215731.43+003757) is a r=19.1 mag galaxy at z=0.391.

J2347+0852: The X-shaped nature of J2347+0852 was brought to our attention by H. Landt (2006, private communication) and the VLA map is published in Landt et al. (2006). It is associated with a z=0.292 quasar (Perlman et al. 1998).

REFERENCES

Adelman-McCarthy, J. K., et al. 2007, ApJS, submitted
Alexander, P., & Leahy, J. P. 1987, MNRAS, 225, 1
Barthel, P. D. 1989, ApJ, 336, 606
Baum, S. A., Heckman, T. M., Bridle, A., van Breugel, W. J. M., & Miley, G. K. 1988, ApJS, 68, 643
Becker, R. H., White, R. L., & Edwards, A. L. 1991, ApJS, 75, 1
Becker, R. H., White, R. L., & Helfand, D. J. 1995, ApJ, 450, 559
Beers, T. C., Gebhardt, K., Forman, W., Huchra, J. P., & Jones, C. 1991, AJ, 102, 1581
Begelman, M. C., Blandford, R. D., & Rees, M. J. 1980, Nature, 287, 307
Best, P. N., Röttgering, H. J. A., & Lehnert, M. D. 1999, MNRAS, 310, 223
Black, A. R. S., Baum, S. A., Leahy, J. P., Perley, R. A., Riley, J. M., & Scheuer, P. A. G. 1992, MNRAS, 256, 186
Blanton, E. L., Gregg, M. D., Helfand, D. J., Becker, R. H., & Leighly, K. M. 2001, AJ, 121, 2915
Boyle, B. J., Shanks, T., Croom, S. M., Smith, R. J., Miller, L., Loaring, N., & Heymans, C. 2000, MNRAS, 317, 1014
Brand, K., Rawlings, S., Hill, G. J., & Tufts, J. R. 2005, MNRAS, 357, 1231
Bridle, A. H., Fomalont, E. B., & Cornwell, T. J. 1981, AJ, 86, 1294
Brinkmann, W., Siebert, J., & Boller, T. 1994, A&A, 281, 355
Canosa, C. M., Worrall, D. M., Hardcastle, M. J., & Birkinshaw, M. 1999, MNRAS, 310, 30
Capetti, A., de Ruiter, H. R., Fanti, R., Morganti, R., Parma, P., & Ulrich, M.-H. 2000, A&A, 362, 871
Capetti, A., Zamfir, S., Rossi, P, Bodo, G., Zanni, C., & Massaglia, S. 2002, A&A, 394, 39
Condon, J. J., Cotton, W. D., Greisen, E. W., Yin, Q. F., Perley, R. A., Taylor, G. B., & Broderick, J. J. 1998, AJ, 115, 1693
Croom, S. M., Smith, R. J., Boyle, B. J., Shanks, T., Loaring, N. S., Miller, L., & Lewis, I. J. 2001, MNRAS, 322, L29
de Ruiter, H. R., Parma, P., Fanti, C., & Fanti, R. 1986, A&AS, 65, 111
Dennett-Thorpe, J., Bridle, A. H., Laing, R. A., & Scheuer, P. A. G. 1999, MNRAS, 304, 271
Dennett-Thorpe, J., Scheuer, P. A. G., Laing, R. A., Bridle, A. H., Pooley, G. G., & Reich, W. 2002, MNRAS, 330, 609
Douglas, J. N., Bash, F. N., Bozyan, F. A., Torrence, G. W., & Wolfe, C. 1996, AJ, 111, 1945
Downes, A. J. B., Peacock, J. A., Savage, A., & Carrie, D. R. 1986, MNRAS, 218, 31
Dunlop, J. S., Peacock, J. A., Savage, A., Lilly, S. J., Heasley, J. N., & Simon, A. J. B. 1989, MNRAS, 238, 1171
Ekers, R. D., Fanti, R., Lari, C., & Parma, P. 1978, Nature, 276, 588
Fairall, A. P., et al. 1992, AJ, 103, 11
Falco, E. E., et al. 1999, PASP, 111, 438
Fanaroff, B. L., & Riley, J. M. 1974, MNRAS, 167, 31P
Fanti, C., Fanti, R., Gioia, I. M., Lari, C., Parma, P., & Ulrich, M. H. 1977, A&AS, 29, 279
Fanti, C., Fanti, R., de Ruiter, H. R., & Parma, P. 1986, A&AS, 65, 145
—. 1987, A&AS, 69, 57
Floyd, D. J. E., Perlman, E., Leahy, J. P., Beswick, R. J., Jackson, N. J., Sparks, W. B., Axon, D. J., & O'Dea, C. P. 2006, ApJ, 639, 23
Gawronski, M. P., Marecki, A., Kunert-Bajraszewska, M., & Kus, A. J. 2005, A&A, 447, 63
Garrington, S. T., Leahy, J. P., Conway, R. G., & Laing, R. A. 1988, Nature, 331, 147
Gizani, N. A. B., & Garrett, M. A. 2002, in Proc. 6th European VLBI Network Symposium, Eds. E. Ros et al., 159-162
González-Serrano, J. I., & Carballo, R. 2000, A&AS, 142, 353
Gopal-Krishna, Biermann, P. L., & Wiita, P. J. 2003, ApJ, 594, L103
Goto, T., et al. 2002, AJ, 123, 1807
Gregory, P. C., & Condon, J. J. 1991, ApJS, 75, 1011
Griffith, M. R., Wright, A. E., Burke, B. F., & Ekers, R. D. 1994, ApJS, 90, 179
—. 1995, ApJS, 97, 347
Haarsma, D. B., et al. 2005, AJ, 130, 1977
Harvanek, M., & Hardcastle, M. J. 1998, ApJS, 119, 25
Heckman, T. M., O'Dea, C. P., Baum, S. A., & Laurikainen, E. 1994, ApJ, 428, 65
Hughes, S. A., & Blandford, R. D. 2003, ApJ, 585, L101
Jackson, N., Roland, J., Bremer, M., Rhee, G., & Webb, J. 1999, A&AS, 134, 401
Jones, D. H., Saunders, W., Read, M. A., & Colless, M. 2005, PASA, 22, 277
Junor, W., Mantovani, F., Morganti, R., & Padrielli, L. 2000, A&AS, 143, 457
Klein, U., Mack, K.-H., Gregorini, L., & Parma, P. 1995, A&A, 303, 427
Komossa, S. 2003, AIP Conf. Proc. 686: The Astrophysics of Gravitational Wave Sources, 686, 161
Kraft, R. P., Hardcastle, M. J., Worrall, D. M., & Murray, S. S. 2005, ApJ, 622, 149
Kunert, M., Marecki, A., Spencer, R. E., Kus, A. J., & Niezgoda, J. 2002, A&A, 391, 47
Lacy, M. 2000, ApJ, 536, L1
Laing, R. A. 1988, Nature, 331, 149
Laing, R. A., & Bridle, A. H. 1987, MNRAS, 228, 557
Laing, R. A., Riley, J. M., & Longair, M. S. 1983, MNRAS, 204, 151
Lal, D. V., & Rao, A. P. 2005, MNRAS, 356, 232
—. 2006, MNRAS, in press (astro-ph/0610678)
Landt, H., Perlman, E.S., & Padovani, P. 2006, ApJ, 637, 183
Leahy, J. P., & Williams, A. G. 1984, MNRAS, 210, 929
Leahy, J. P., Pooley, G. G., & Riley, J. M. 1986, MNRAS, 222, 753
Leahy, J. P., & Perley, R. A. 1991, AJ, 102, 537
Leahy, J. P., & Parma, P. 1992, Extragalactic Radio Sources. From Beams to Jets, J. Roland, H. Sol, & G. Pelletier, eds. (Cambridge: Cambridge UP) 307
Leahy, J. P., Black, A. R. S., Dennett-Thorpe, J., Hardcastle, M. J., Komissarov, S., Perley, R. A., Riley, J. M., & Scheuer, P. A. G. 1997, MNRAS, 291, 20
Ledlow, M. J., & Owen, F. N. 1996, AJ, 112, 9
Ledlow, M. J., Voges, W., Owen, F. N., & Burns, J. O. 2003, AJ, 126, 2740
Lehár, J., Buchalter, A., McMahon, R. G., Kochanek, C. S., & Muxlow, T. W. B. 2001, ApJ, 547, 60
Liu, F. K. 2004, MNRAS, 347, 1357
Machalski, J., & Condon, J. J. 1983, AJ, 88, 1591
—. 1999, ApJS, 123, 41
Mack, K.-H., Gregorini, L., Parma, P., & Klein, U. 1994, A&AS, 103, 157
Madau, P., & Quataert, E. 2004, ApJ, 606, L17
Maddox, S. J., Efstathiou, G., Sutherland, W. J., & Loveday, J. 1990, MNRAS, 243, 692

Maness, H. L., Taylor, G. B., Zavala, R. T., Peck, A. B., & Pollack, L. K. 2004, ApJ, 602, 123
Mantovani, F., Junor, W., Fanti, R., Padrielli, L., Browne, I. W. A., & Muxlow, T. W. B. 1992, MNRAS, 257, 353
Marecki, A., Thomasson, P., Mack, K.-H., & Kunert-Bajraszewka, M. 2006, A&A, 448, 479
McMahon, R. G., White, R. L., Helfand, D. J., & Becker, R. H. 2002, ApJS, 143, 1
Merritt, D., & Ekers, R. D. 2002, Science, 297, 1310
Miley, G. K., & Osterbrock, D. E. 1979, PASP, 91, 257
Miller, N. A., & Owen, F. N. 2001, ApJS, 134, 355
Miller, N. A., Ledlow, M. J., Owen, F. N., & Hill, J. M. 2002, AJ, 123, 3018
Monet, D. G., et al. 2003, AJ, 125, 984
Murgia, M., Parma, P., de Ruiter, H. R., Bondi, M., Ekers, R. D., Fanti, R., & Fomalont, E. B. 2001, A&A, 380, 102
Murphy, D. W., Browne, I. W. A., & Perley, R. A. 1993, MNRAS, 264, 298
Myers, S. T., & Spangler, S. R. 1985, ApJ, 291, 52
O' Dea, C. P., & Owen, F. N. 1985, AJ, 90, 927
O'Dea, C. P. 1998, PASP, 110, 493
Orr, M. J. L. & Browne, I. W. A. 1982, MNRAS, 200, 1067
Owen, F. N., White, R. A., & Burns, J. O. 1992, ApJS, 80, 501
Owen, F. N., Ledlow, M. J., & Keel, W. C. 1995, AJ, 109, 14
Owen, F. N., & Ledlow, M. J. 1997, ApJS, 108, 41
Parma, P., Ekers, R. D., & Fanti, R. 1985, A&AS, 59, 511
Parma, P., de Ruiter, H. R., Fanti, C., & Fanti, R. 1986, A&AS, 64, 135
Perlman, E. S., Padovani, P., Giommi, P., Sambruna, R., Jones, L. R., Tzioumis, A., & Reynolds, J. 1998, AJ, 115, 1253
Perryman, M. A. C., Lilly, S. J., Longair, M. S., & Downes, A. J. B. 1984, MNRAS, 209, 159
Proctor, D. D. 2003, J. Electron. Imaging, 12, 398
—. 2006, ApJS, 165, 95
Reid, R. I., Kronberg, P. P., & Perley, R. A. 1999, ApJS, 124, 285
Rines, K., Geller, M. J., Kurtz, M. J., & Diaferio, A. 2003, AJ, 126, 2152
Rottmann, H. 2001, PhD Thesis, Univ. of Bonn (http://hss.ulb.uni-bonn.de/ulb_bonn/diss_online/math_nat_fak/2001/rottmann_helge/)
Sandage, A. 1966, ApJ, 145, 1
—. 1972, ApJ, 178, 25
Schmidt, M. 1965, ApJ, 141, 1
Schneider, D. P., et al. 2002, AJ, 123, 567
Slinglend, K., Batuski, D., Miller, C., Haase, S., Michaud, K., & Hill, J. M. 1998, ApJS, 115, 1
Smith, H. E., Spinrad, H., & Smith, E. O. 1976, PASP, 88, 621
Smith, H. E., & Spinrad, H. 1980, PASP, 92, 553
Snellen, I. A. G., McMahon, R. G., Hook, I. M., & Browne, I. W. A. 2002, MNRAS, 329, 700
Spangler, S. R., & Sakurai, T. 1985, ApJ, 297, 84
Spinrad, H., Hunstead, R. W., & Kron, R. G. 1979, ApJS, 41, 701
Spinrad, H., Marr, J., Aguilar, L., & Djorgovski, S. 1985, PASP, 97, 932
Struble, M. F., & Rood, H. J. 1999, ApJS, 125, 35
Ulrich, M.-H., & Roennback, J. 1996, A&A, 313, 750
van Breugel, W., & Jagers, W. 1982, A&AS, 49, 529
van Breugel, W., Helfand, D., Balick, B., Heckman, T., & Miley, G. 1983, AJ, 88, 40
Vigotti, M., Vettolani, G., Merighi, R., Lahulla, J. F., & Lopez-Arroyo, M. 1990, A&AS, 83, 205
Wang, T.-G., Zhou, H.-Y., & Dong, X.-B. 2003, AJ, 126, 113
Werner, P. N., Worrall, D. M., & Birkinshaw, M. 1999, MNRAS, 307, 722
Willott, C. J., Rawlings, S., Jarvis, M. J., & Blundell, K. M. 2003, MNRAS, 339, 173
Wolter, A., & Celotti, A. 2001, A&A, 371, 527
Worrall, D.M., Birkinshaw, M. & Cameron, R.A. 1995, ApJ, 449, 93
Worrall, D. M., & Birkinshaw, M. 2000, ApJ, 530, 719
Wright, A. & Otrupcek, R. 1990, Parkes Catalogue, Australia Telescope National Facility
Zakamska, N. L., Strauss, M. A., Heckman, T. M., Ivezić, Ž., & Krolik, J. H. 2004, AJ, 128, 1002
Zickgraf, F.-J., Engels, D., Hagen, H.-J., Reimers, D., & Voges, W. 2003, A&A, 406, 535
Zier, C. 2005, MNRAS, 364, 583
Zirbel, E. L. 1997, ApJ, 476, 489
Zwicky, F., Karpowicz, M., & Kowal, C. T. 1965, "Catalogue of Galaxies and of Clusters of Galaxies," Vol. V (Pasadena: California Institute of Technology)

TABLE A1

LIST OF KNOWN X-SHAPED* RADIO SOURCES

J2000 Name (1)	Other (2)	z (3)	Ref. (4)	$F_{1.4}$ (5)	Radio maps (6)	Leahy (7)	Rottmann (8)	Capetti (9)	FIRST ID? (10)	NVSS ID? (11)	Notes (12)
J0009+1244	4C+12.03	0.156*	P84	1982	L91,L06	✓	✓	✓	..	Yes	
J0058+2651	NGC326, B2 0055+26	0.0477	W99	1782	E78,M01	✓	✓	..	..	Yes	Double Galaxy
J0148+5332	3C52	0.2854	S85	3910	L84,L86,A87,L06	✓	✓	✓	..	No	
J0220–0156	3C63	0.175	S80	3531	B88,H98	..	..	✓	Yes	No	
J0516+2458	3C136.1	0.064	S85	3073	L84,L86,A87,L06	✓	✓	✓	..	Yes	
J0805+2409*	3C192	0.0598	S66	5158	B88,L97,D99,L06	..	..	✓	r	No	Small wings
J0831+3219	4C+32.25, B2 0828+32	0.0507	D86	1886	P85,F87,M94,K95,L06	✓	✓	✓	r	Yes	
J0941+3944	3C223.1	0.1075	S66	2034	B92,D02,L05	✓	✓	✓	Yes	Yes	
J1020+4831	4C+48.29	0.052	M79	1727	V82,L06	✓	..	..	r	Yes	
J1101+1640	Abell 1145, 1059+169	0.0680	O97	640	O92,O97,L06	✓	..	..	r	Yes	
J1130+0058	4C+01.30	0.1325	W03	675	W03	..	..	..	Yes	No	Quasar
J1206+0406	4C+04.40, 1203+043	..	..	1501	M92,J00	..	..	..	Yes	No	
J1357+4807	..	0.383	C06	288	L01	..	..	..	No	No	
J1513+2607	3C315	0.1083	S65	4329	L84,L86,A87,L06	✓	✓	✓	Yes	Yes	Double Galaxy
J1824+7420*	3C379.1	0.2560	S76	1879	M85,Spa85	..	✓	..	..	No	Small wings
J1952+0230	3C403	0.059	S72	5900	B92,D02,K05,L06	✓	✓	✓	..	Yes	
J2123+2504	3C433	0.1016	S65	11940	V83,B92,L06	✓	..	..	..	No	
J2157+0037	..	0.3907	Z04	242	Z04	..	..	..	p,s	Yes	
J2347+0852	..	0.292	P98	155	Lan06	..	..	..	..	No	Quasar

Note. — The asterick (*) denotes the two sources with shorter winged structures than the other bona-fide X-shaped sources. As these were included in the known lists of X-sources, we list them here with the aim of summarizing these works.

Note. — (1, 2): Names based on J2000.0 coordinates and other common catalogue names.

Note. — (3, 4): Redshift (z) and original references. A new redshift was determined for J1357+4807 (see references). *Several works (e.g., Heckman et al. 1994; Rottmann 2001; Merritt & Ekers 2002) list this object as z=0.110, which was estimated from the object's apparent r-magnitude by Laing et al. (1983). The quoted value here is derived from spectroscopic measurements of emission lines.

Note. — (5): Radio 1.4 GHz radio flux density (mJy).

Note. — (6): Representative radio maps from the literature. See Rottmann (2001) for additional maps of sources from his list.

Note. — (7, 8, 9): Indicates objects appearing in the lists of Leahy & Parma (1992) (as given in Merritt & Ekers (2002)), Rottmann (2001), and Capetti et al. (2002).

Note. — (10, 11): Indicates whether the X-shaped morphologies were distinguishable in the FIRST and NVSS maps. In the FIRST column, the codes, p and s, meant it failed to meet one or both of our search criteria: p=peak below threshold of 5 mJy/bm, but size large enough; s=size smaller than 5″ threshold, but peak high enough. r= did meet both of our search criteria but the overall source angular size is too large and much of the diffuse emission was resolved out in the FIRST map. See § 5.1 for a description.

Note. — References: A87=Alexander & Leahy (1987), B88=Baum et al. (1988), B92=Black et al. (1992), C06=C.C. Cheung & S.E. Healey (2006, unpublished) – see Appendix, D86=de Ruiter et al. (1986), D99=Dennett-Thorpe et al. (1999), D02=Dennett-Thorpe et al. (2002), E78=Ekers et al. (1978), F87=Fanti et al. (1987), H98=Harvanek & Hardcastle (1998), J00=Junor et al. (2000), K95=Klein et al. (1995), K05=Kraft et al. (2005), L84=Leahy & Williams (1984), L86=Leahy et al. (1986), L91=Leahy & Perley (1991), L97=Leahy et al. (1997), L04=Lehár et al. (2001), L05=Lal & Rao (2005), L06=Lal & Rao (2006), Lan06=Landt et al. (2006), M79=Miley & Osterbrock (1979), M85=Myers & Spangler (1985), M92=Mantovani et al. (1992), M94=Mack et al. (1994), M01=Murgia et al. (2001), O92=Owen et al. (1992), O97=Owen & Ledlow (1997), P84=Perryman et al. (1984), P85=Parma et al. (1985), P98=Perlman et al. (1998), S65=Schmidt (1965), S66=Sandage (1966), S72=Sandage (1972), S76=Smith, Spinrad, & Smith (1976), S80=Smith & Spinrad (1980), Spa85=Spangler & Sakurai (1985), S85=Spinrad et al. (1985), V82=van Breugel & Jagers (1982), V83=van Breugel et al. (1983), W99=Werner et al. (1999), W03=Wang et al. (2003), Z04=Zakamska et al. (2004).

TABLE A2

CANDIDATE X-SHAPED RADIO SOURCES FROM FIRST

Catalog Number	Name	R.A. (J2000.0)	Dec. (J2000.0)	mag.	$g-r$	Ref.	ID	z	Ref.	$F_{0.365}$ [mJy]	$F_{1.4}$ [mJy]	$F_{4.9}$ [mJy]	Ref.$_{4.9}$	$\alpha_{1.4}^{0.365}$	$\alpha_{4.9}^{1.4}$	Other Catalogs
(1)	(2)	(3)	(4)	(5)	(6)	(7)	(8)	(9)	(10)	(11)	(12)	(13)	(14)	(15)	(16)	(17)
1	J0001–0033	00 01 40.18	–00 33 50.6	17.4	1.5	SDSS	G	0.2469	SDSS	..	73	50	PMN	..	0.30	
2	J0033–0149	00 33 02.41	–01 49 56.6	14.1*	..	USNO	G	0.1301	6dF	169	87	..	..	0.49	..	
3	J0036+0048	00 36 36.21	+00 48 53.4	20.4	1.2	SDSS	..	..	..	758	280	89	PMN	0.74	0.91	
4	J0045+0021	00 45 42.11	+00 21 05.5	21.5	..	D89	..	..	..	1677	509	159	PMN	0.89	0.93	4C-00.05, PKS
5	J0049+0059	00 49 39.45	+00 59 53.8	18.1	1.7	SDSS	G	0.3044	SDSS	427	155	77	PMN	0.75	0.56	
6	J0113+0106	01 13 41.11	+01 06 08.5	18.1	1.3	SDSS	G	0.281	L00	..	391	121	PMN	..	0.94	
7	J0115–0000	01 15 27.37	–00 00 01.5	20.5	1.4	SDSS	G	0.381	L00	..	222	54	B91	..	1.13	4C-00.07, PKS
8	J0143–0119	01 43 16.75	–01 19 00.8	19.3	..	USNO	G	0.520	L00	1978	823	340	PMN	0.65	0.71	4C-01.09, PKS
9	J0144–0830	01 44 09.98	–08 30 02.8	18.6	1.2	SDSS	..	..	..	..	47	..	..	..	..	
10	J0145–0159	01 45 19.99	–01 59 47.9	13.4*	..	USNO	G	0.1264	6dF	472	272	97	PMN	0.41	0.82	
11	J0147–0851	01 47 19.28	–08 51 19.6	20.2	1.1	SDSS	..	..	..	839	306	115	PMN	0.75	0.78	
12	J0211–0920	02 11 46.96	–09 20 36.6	18.5	1.3	SDSS	..	..	..	377	180	..	..	0.55	..	
13	J0225–0738	02 25 08.62	–07 38 49.1	24.3	0.5	SDSS	..	..	..	916	318	131	PMN	0.79	0.71	PKS
14	J0702+5002	07 02 47.92	+50 02 05.3	15.5*	..	USNO	G	0.0946	H05	761	334	115	G91	0.61	0.85	6C
15	J0725+5835	07 25 32.27	+58 35 27.4	19.9	..	USNO	..	..	..	450	178	45	G91	0.69	1.10	6C, 8C
16	J0805+4854	08 05 44.0	+48 54 58	..	..	FIRST	..	..	..	..	34	..	..	..	..	
17	J0813+4347	08 13 00.11	+43 47 48.5	16.1	1.1	SDSS	G	0.1282	SDSS	624	333	156	G91	0.47	0.61	6C, B3
18	J0821+2922	08 21 49.60	+29 22 44.4	20.2	0.9	SDSS	G	0.246	W03	478	117	27	G91	1.05	1.17	5C07.178, B2
19	J0836+3125	08 36 35.46	+31 25 51.2	19.8	2.0	SDSS	..	..	..	524	291	111	G91	0.44	0.77	6C
20	J0838+3253	08 38 44.61	+32 53 11.8	16.9	1.4	SDSS	G	0.2127	SDSS	..	121	60	G91	..	0.56	6C
21	J0845+4031	08 45 08.40	+40 31 15.4	18.8	1.5	SDSS	..	..	..	448	164	66	G91	0.75	0.73	6C, B3
22	J0846+3956	08 46 03.58	+39 56 57.9	20.8	1.0	SDSS	..	..	..	665	197	59	G91	0.90	0.96	6C, B3
23	J0859–0433	08 59 50.19	–04 33 06.9	18.8	..	USNO	..	..	..	454	237	105	PMN	0.48	0.65	
24	J0914+1715	09 14 05.21	+17 15 54.3	19.7	1.3	SDSS	..	..	..	4612	1527	558	G91	0.82	0.80	4C+17.48, PKS
25	J0917+0523	09 17 44.31	+05 23 10.1	20.3	1.2	SDSS	..	..	..	1798	612	218	PMN	0.80	0.82	4C+05.39, PKS
26	J0924+4233	09 24 46.98	+42 33 47.1	17.8	1.4	SDSS	G	0.2274	SDSS	636	292	105	G91	0.58	0.82	6C, B3
27	J0941–0143	09 41 22.58	–01 43 01.1	17.8	..	USNO	G	0.382	S79	1844	830	359	PMN	0.59	0.67	4C-01.19, PKS
28	J0941+2147	09 41 58.31	+21 47 44.2	22.6	1.5	SDSS	..	..	..	704	206	74	G91	0.91	0.82	7C
29	J0943+2834	09 43 02.25	+28 34 45.8	20.6	1.0	SDSS	..	..	..	1731	647	187	G91	0.73	0.99	4C+28.23, 7C, 9C
30	J1005+1154	10 05 52.53	+11 54 37.0	16.3	1.2	SDSS	G	0.1656	SDSS	437	205	67	G91	0.56	0.89	
31	J1008+0030	10 08 11.43	+00 30 00.0	15.8	0.9	SDSS	G	0.0977	O95	534	484	259	PMN	0.07	0.50	Abell 0933, PKS
32	J1015+5944	10 15 41.14	+59 44 45.2	18.3	-0.1	SDSS	Q	0.5271	SDSS	732	221	73	G91	0.89	0.88	6C, 8C
33	J1040+5056	10 40 22.48	+50 56 25.1	17.1	1.1	SDSS	G	0.1539	SDSS	565	194	113	G91	0.80	0.43	6C
34	J1043+3131	10 43 18.63	+31 31 06.1	14.8	0.8	SDSS	G	0.0357	F99,SDSS	1243	749	377	G91	0.38	0.55	6C, 7C, B2
35	J1049+4422	10 49 35.28	+44 22 04.0	20.3	1.1	SDSS	..	..	..	461	144	60	G91	0.87	0.70	6C, B3
36	J1054+5521	10 54 00.6	+55 21 53	..	..	FIRST	..	..	..	496	222	80	G91	0.60	0.81	6C, 7C
37	J1055–0707	10 55 52.56	–07 07 19.1	17.6	..	USNO	..	..	..	1689	651	213	PMN	0.71	0.89	4C-06.26, PKS
38	J1102+0250	11 02 06.56	+02 50 45.7	22.3	1.0	SDSS	..	..	..	1626	506	167	PMN	0.87	0.88	4C+03.20, PKS
39	J1111+4050	11 11 39.74	+40 50 24.1	14.8	0.9	SDSS	G	0.0737	SDSS	2212	819	263	G91	0.74	0.91	4C+41.23, B3
40	J1114+2632	11 14 27.10	+26 32 58.8	21.0	0.6	SDSS	..	..		568	232	165	G91	0.67	0.27	7C
41	J1120+4354	11 20 16.18	+43 54 51.4	20.4	1.4	SDSS	..	..	..	1103	406	152	G91	0.74	0.78	6C, B3
42	J1128+1919	11 28 37.7	+19 19 57	..	..	FIRST	..	..	..	277	125	48	G91	0.59	0.76	
43	J1135–0737	11 35 36.78	–07 37 00.1	19.2	..	USNO	..	..	..	..	106	..	..	..	..	
44	J1140+1057	11 40 49.70	+10 57 56.3	16.6	0.9	SDSS	G	0.0808	SDSS	1067	537	212	G91	0.51	0.74	
45	J1200+6105	12 00 06.00	+61 05 44.5	18.3	1.1	SDSS	..	..	..	742	278	82	G91	0.73	0.97	6C, 8C
46	J1201–0703	12 01 25.76	–07 03 11.0	16.4	..	USNO	..	..	..	330	203	63	PMN	0.36	0.93	
47	J1202+4915	12 02 35.10	+49 15 31.7	21.1	1.6	SDSS	..	..	..	..	104	31	B91	..	0.97	6C
48	J1206+3812	12 06 17.35	+38 12 34.9	18.4	0.2	SDSS	Q	0.838	V90,SDSS	885	247	62	G91	0.95	1.10	6C, B3
49	J1207+3352	12 07 32.92	+33 52 40.1	15.2	0.8	SDSS	G	0.0788	F87,SDSS	1101	490	225	G91	0.60	0.62	6C, 7C, B2
50	J1210–0341	12 10 18.77	–03 41 53.3	17.8	1.2	SDSS	G	0.26	M99	267	151	..	..	0.42	..	

TABLE A2—*Continued*

Catalog Number (1)	Name (2)	R.A. (J2000.0) (3)	Dec. (J2000.0) (4)	mag. (5)	$g-r$ (6)	Ref. (7)	ID (8)	z (9)	Ref. (10)	$F_{0.365}$ [mJy] (11)	$F_{1.4}$ [mJy] (12)	$F_{4.9}$ [mJy] (13)	Ref.$_{4.9}$ (14)	$\alpha_{1.4}^{0.365}$ (15)	$\alpha_{4.9}^{1.4}$ (16)	Other Catalogs (17)
51	J1210+1121	12 10 11.99	+11 21 02.7	16.6	1.4	SDSS	G	0.1963	SDSS	..	133	45	G91	..	0.87	
52	J1211+4539	12 11 02.50	+45 39 14.4	22.0	1.1	SDSS	..	..	..	716	232	73	G91	0.84	0.92	6C, B3
53	J1218+1955	12 18 59.15	+19 55 28.0	19.9	1.3	SDSS	..	..	..	2868	1047	269	G91	0.75	1.08	4C+20.28, 7C, PKS
54	J1227–0742	12 27 12.5	–07 42 00	..	..	FIRST	..	..	..	427	168	..	..	0.69	..	
55	J1227+2155	12 27 49.45	+21 55 19.6	19.7	1.7	SDSS	..	..	..	770	199	45	G91	1.01	1.19	7C
56	J1228+2642	12 28 03.83	+26 42 26.7	17.8	1.3	SDSS	..	..	..	473	185	92	G91	0.70	0.56	7C
57	J1232–0717	12 32 52.50	–07 17 28.9	19.7	..	USNO	..	..	..	1369	512	160	PKS	0.73	0.93	PKS
58	J1247+4646	12 47 26.84	+46 46 06.0	22.3	2.9*	SDSS	..	..	..	451	135	29	G91	0.90	1.23	6C, B3
59	J1253+3435	12 53 24.29	+34 35 18.2	19.1	1.5	SDSS	..	..	..	776	362	119	G91	0.57	0.89	5C, 6C, 7C, B2
60	J1258+3227	12 58 32.87	+32 27 40.8	17.0	1.1	SDSS	..	..	..	..	149	63	G91	..	0.69	5C, 6C, 7C
61	J1309–0012	13 09 49.74	–00 12 35.6	19.4	0.7	SDSS	G	0.419	B99	4525	1637	470	PKS	0.76	1.00	4C+00.46, PKS
62	J1310+5458	13 10 15.40	+54 58 34.2	19.2	1.2	SDSS	..	..	..	706	226	93	G91	0.85	0.71	6C
63	J1316+2427	13 16 38.27	+24 27 32.4	19.6	1.0	SDSS	..	..	..	..	75	..	..	..	..	7C
64	J1327–0203	13 27 38.22	–02 03 09.9	16.6	1.3	SDSS	G	0.1828	SDSS	3471	1179	470	PKS	0.80	0.73	4C-01.29, PKS
65	J1330–0206	13 30 10.32	–02 06 18.0	15.5	1.0	SDSS	G	0.0866	SDSS	526	159	..	..	0.89	..	
66	J1339–0016	13 39 34.23	–00 16 35.5	15.9	1.2	SDSS	G	0.1452	SDSS	..	207	120	PKS	..	0.44	PKS
67	J1342+2547	13 42 45.32	+25 47 11.5	20.2	0.4	SDSS	..	..	..	910	365	114	G91	0.68	0.93	7C
68	J1345+5233	13 45 41.64	+52 33 35.6	20.7	1.4	SDSS	..	..	..	..	71	30	B91	..	0.69	6C
69	J1348+4411	13 48 04.59	+44 11 24.2	18.5	1.4	SDSS	..	..	..	..	158	98	G91	..	0.38	6C, B3
70	J1351+5559	13 51 42.14	+55 59 43.1	15.1	1.0	SDSS	..	..	..	286	221	73	G91	0.19	0.88	6C, 8C
71	J1353+0724	13 53 06.37	+07 24 37.1	19.3	1.3	SDSS	..	..	..	852	294	114	PMN	0.79	0.76	
72	J1406–0154	14 06 48.61	–01 54 16.5	20.9	1.8	SDSS	..	..	..	3521	1143	300	PKS	0.84	1.07	4C-01.31, PKS
73	J1406+0657	14 06 02.41	+06 57 15.7	18.5	0.0	SDSS	..	..	..	896	339	119	PMN	0.72	0.84	
74	J1408+0225	14 08 28.41	+02 25 50.3	18.4	1.1	SDSS	..	..	..	573	244	..	..	0.64	..	
75	J1411+0907	14 11 21.14	+09 07 35.4	20.4	4.2*	SDSS	..	..	..	..	260	72	PMN	..	1.02	
76	J1424+2637	14 24 40.53	+26 37 30.5	14.0	0.8	SDSS	G	0.0372	M02	852	857	344	G91	0.00	0.73	7C, B2, PKS
77	J1430+5217	14 30 17.34	+52 17 35.0	19.4	1.1	SDSS	Q	0.3671	SDSS	1775	671	217	G91	0.72	0.90	6C
78	J1433+0037	14 33 51.87	+00 37 23.4	19.8	1.8	SDSS	..	..	..	669	275	97	PMN	0.66	0.83	
79	J1434+5906	14 34 02.17	+59 06 53.3	20.9	1.9	SDSS	..	..	..	682	315	115	G91	0.57	0.80	6C, 8C
80	J1437+0834	14 37 38.90	+08 34 22.1	19.2	1.2	SDSS	..	..	..	548	208	99	PMN	0.72	0.59	
81	J1444+4147	14 44 07.25	+41 47 50.3	17.3	1.2	SDSS	G	0.1880	SDSS	354	372	147	G91	-0.04	0.74	6C, B3
82	J1454+2732	14 54 42.22	+27 32 11.8	20.2	2.1	SDSS	..	..	..	617	211	73	G91	0.80	0.85	7C
83	J1455+3237	14 55 58.28	+32 37 32.5	15.9	0.9	SDSS	G	0.084	SDSS	249	107	35	G91	0.63	0.89	6C, 7C
84	J1456+2542	14 56 43.16	+25 42 17.5	20.6	1.7	SDSS	..	..	..	..	36	..	..	..	..	
85	J1459+2903	14 59 41.95	+29 03 31.8	16.5	1.1	SDSS	G	0.1460	G00	..	367	170	G91	..	0.61	7C, B2
86	J1501+0752	15 01 57.44	+07 52 26.7	20.9	1.5	SDSS	..	..	..	1562	509	170	PMN	0.83	0.88	4C+08.43
87	J1515–0532	15 15 33.66	–05 32 51.0	19.9	..	APM	..	..	..	3070	920	289	PMN	0.90	0.92	
88	J1522+4527	15 22 13.1	+45 27 57	..	..	FIRST	..	..	..	..	107	39	G91	..	0.81	6C, B3
89	J1537+2648	15 37 07.33	+26 48 23.2	18.3	1.5	SDSS	..	..	..	647	263	111	G91	0.67	0.69	7C
90	J1600+2058	16 00 38.95	+20 58 51.7	17.2	1.3	SDSS	..	..	..	1214	523	185	G91	0.63	0.83	7C
91	J1603+5242	16 03 44.96	+52 42 20.6	17.9	1.1	SDSS	..	..	..	..	348	108	G91	..	0.93	6C
92	J1606+0000	16 06 12.68	+00 00 27.1	15.0	1.0	SDSS	G	0.059	B99	5131	2385	1090	PMN	0.57	0.63	4C+00.58, PKS
93	J1606+4517	16 06 38.88	+45 17 37.1	20.5	1.3	SDSS	..	..	..	383	116	36	G91	0.89	0.93	B3
94	J1614+2817	16 14 28.40	+28 17 31.0	15.9	1.0	SDSS	G	0.1069	M01	565	424	169	G91	0.21	0.73	
95	J1625+2705	16 25 30.68	+27 05 46.3	18.5	-0.1	SDSS	Q	0.5259	SDSS	1734	531	245	G91	0.88	0.62	B3
96	J1653+3115	16 53 37.31	+31 15 27.5	20.6	1.1	SDSS	..	..	..	335	213	104	G91	0.34	0.57	6C
97	J1655+4551	16 55 16.2	+45 51 08	..	..	DSS	..	..	..	..	78	..	..	..	..	6C, B3
98	J1656+3952	16 56 36.65	+39 52 58.3	18.9	1.7	SDSS	..	..	..	395	147	71	G91	0.74	0.58	6C, B3
99	J2226+0125	22 26 45.6	+01 25 11	..	..	FIRST	..	..	..	..	81	46	G91	..	0.45	
100	J2359–1041	23 59 46.47	–10 41 15.4	18.9	1.0	SDSS	..	..	..	710	280	102	PMN	0.69	0.81	

TABLE A2—*Continued*

Catalog Number	Name	R.A. (J2000.0)	Dec. (J2000.0)	mag.	$g-r$	Ref.	ID	z	Ref.	$F_{0.365}$ [mJy]	$F_{1.4}$ [mJy]	$F_{4.9}$ [mJy]	Ref.$_{4.9}$	$\alpha_{1.4}^{0.365}$	$\alpha_{4.9}^{1.4}$	Other Catalogs
(1)	(2)	(3)	(4)	(5)	(6)	(7)	(8)	(9)	(10)	(11)	(12)	(13)	(14)	(15)	(16)	(17)

Note. — (2, 3, 4): Name based on J2000.0 equinox positions in right ascension (R.A.) and declination (Dec.). Positions are of the optical counterparts when identified in the SDSS (most widely adopted), USNO, and APM catalogs, or other published works (see Column 7). When the optical counterparts were not catalogued, less precise positions were estimated directly from the DSS or FIRST images (Figure A4).

Note. — (5, 6, 7): Observed optical magnitudes (mag.) in the r-band. SDSS model magnitudes were preferred whenever available. USNO magnitudes are valid for point sources only so obviously extended objects in the DSS images are marked with an asterisk (*). SDSS $g-r$ colors are listed when available and anomalously large $g-r$ values are indicated (*). Inspection of SDSS data at their five-bands show inconsistent g-band magnitudes in these cases: more reliable colors are $u-r$=1.7 (J1247+4646) and 2.2 (J1411+0907).

Note. — (8, 9, 10): Spectroscopic identifications (ID; G=radio galaxy, Q=quasar), redshifts (z) and references.

Note. — (11, 12, 13, 14): Integrated radio flux density measurements at 365 MHz from the TXS survey, 1.4 GHz from NVSS, and at 4.9 GHz from the references listed in column (14): Green Bank (B91 and G91), PMN, or PKS catalogs. See § 3.3 for further explanation.

Note. — (15, 16): Spectral index (α) calculated between 365 MHz and 1.4 GHz (column 15) and between 1.4 and 4.9 GHz (column 16) where $F_\nu \propto \nu^{-\alpha}$.

Note. — (17): Other names and (mostly radio; the Cambridge, 4C, 5C, 6C, 7C, 8C, and, Bologna, B2 and B3) catalogs in which these objects appear.

Note. — References: B99=Best et al. (1999), D89=Dunlop et al. (1989), F87=Fanti et al. (1987), F99=Falco et al. (1999), G00=González-Serrano & Carballo (2000), H05=S.E. Healey (2005, private communication), L00=Lacy (2000), M99=Machalski & Condon (1999), M01=Miller & Owen (2001), M02=Miller et al. (2002), O95=Owen et al. (1995), S79=Spinrad et al. (1979), V90=Vigotti et al. (1990), W03=Willott et al. (2003).

Note. — Catalogs: 6dF=Jones et al. (2005), APM=Maddox et al. (1990), SDSS=Adelman-McCarthy et al. (2007), USNO=Monet et al. (2003), FIRST=Becker et al. (1995), Green Bank: B91=Becker, White, & Edwards (1991) and G91=Gregory & Condon (1991), NVSS=Condon et al. (1998), PMN=Griffith et al. (1994, 1995), PKS=Wright & Otrupcek (1990), TXS=Douglas et al. (1996).

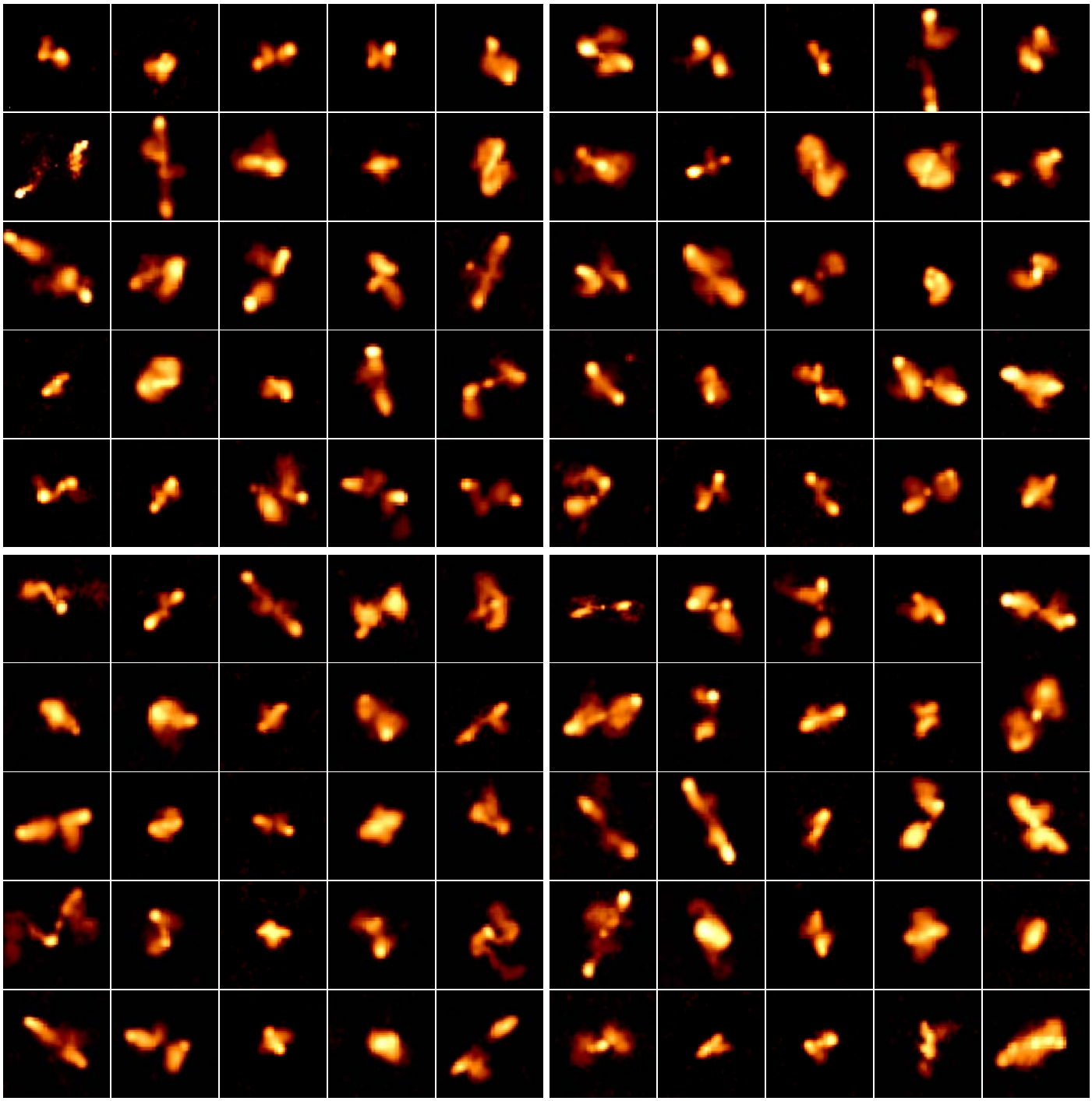

FIG. A1.— Color thumbnail images of the 100 FIRST X-shaped radio source candidates. The objects are ordered in increasing R.A. order (refer to the catalog numbers in Table A2) from left to right then down within each of the four 5×5 panels (top left = cat. no. 1–25, top right = cat. no. 26–50, bottom left = cat no. 51–75, bottom right = cat. no. 76–100). See Figure A4 for image scales.

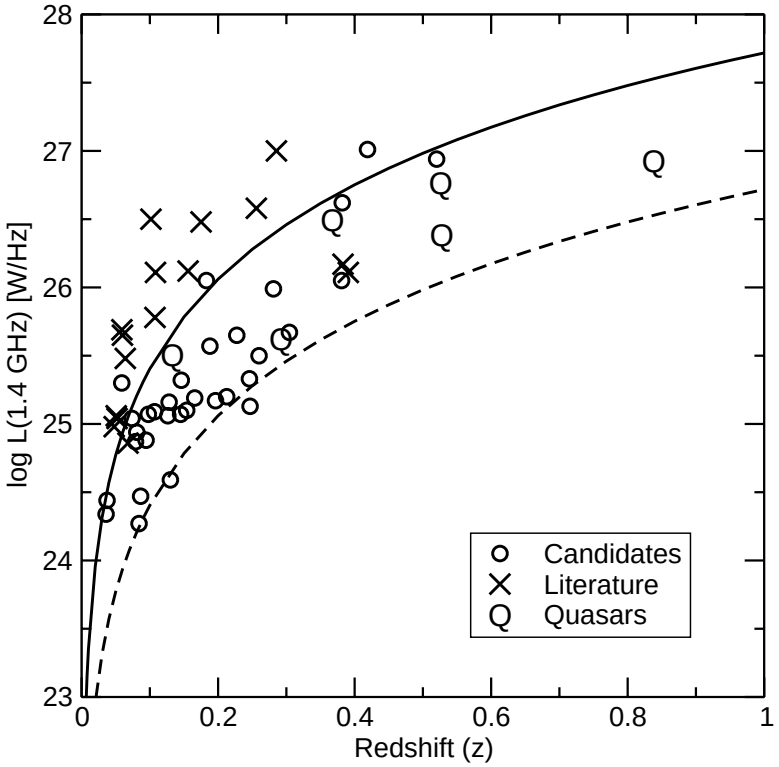

FIG. A2.— The 1.4 GHz radio luminosity–redshift distribution of the spectroscopically identified candidate (circles) and known (crosses) X-shaped radio sources. Quasars are denoted with the letter Q (those at z>0.3 were identified by us). The solid and dashed lines represent the corresponding luminosity of a 1 Jy and 100 mJy radio source, respectively.

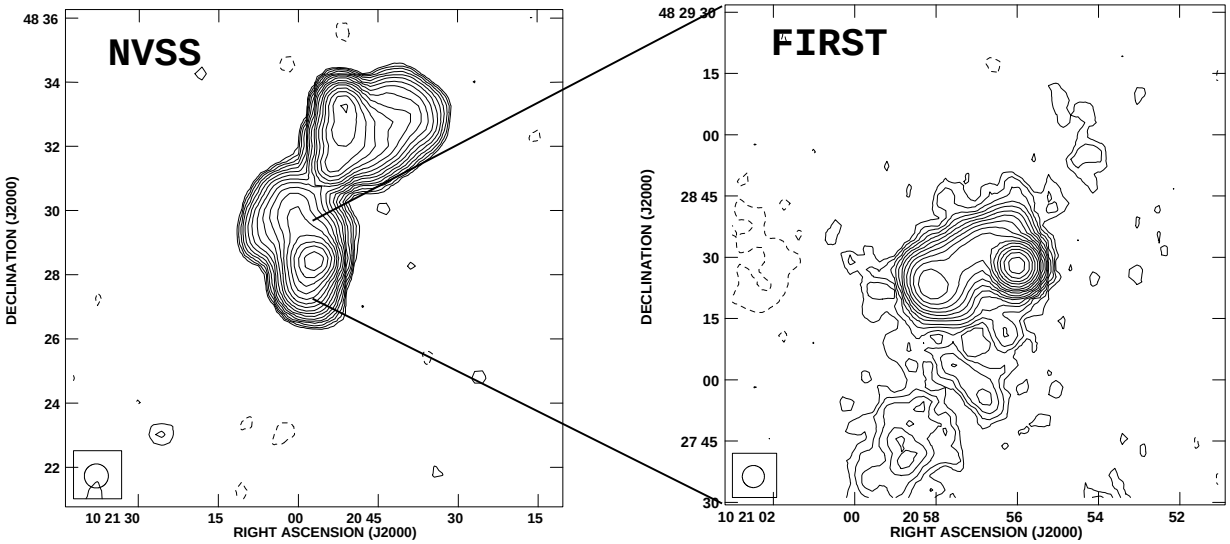

FIG. A3.— Example of a FIRST image field [right panel] initially identified as an X-shaped radio source candidate (imagined as east-west lobes and winged emission to the south). A lower resolution map from NVSS [left panel] revealed this to be a hot spot complex in the southern lobe of 4C+48.29, coincidentally, a known X-shaped radio source (Table A1). The restoring beams of 45″ (left) and 5.4″ (right) are shown to the bottom left of each panel. The contour levels begin at 1.25 and 0.35 mJy/bm up to peaks of 294.7 and 81.8 mJy/bm, respectively, increasing by $\sqrt{2}$.

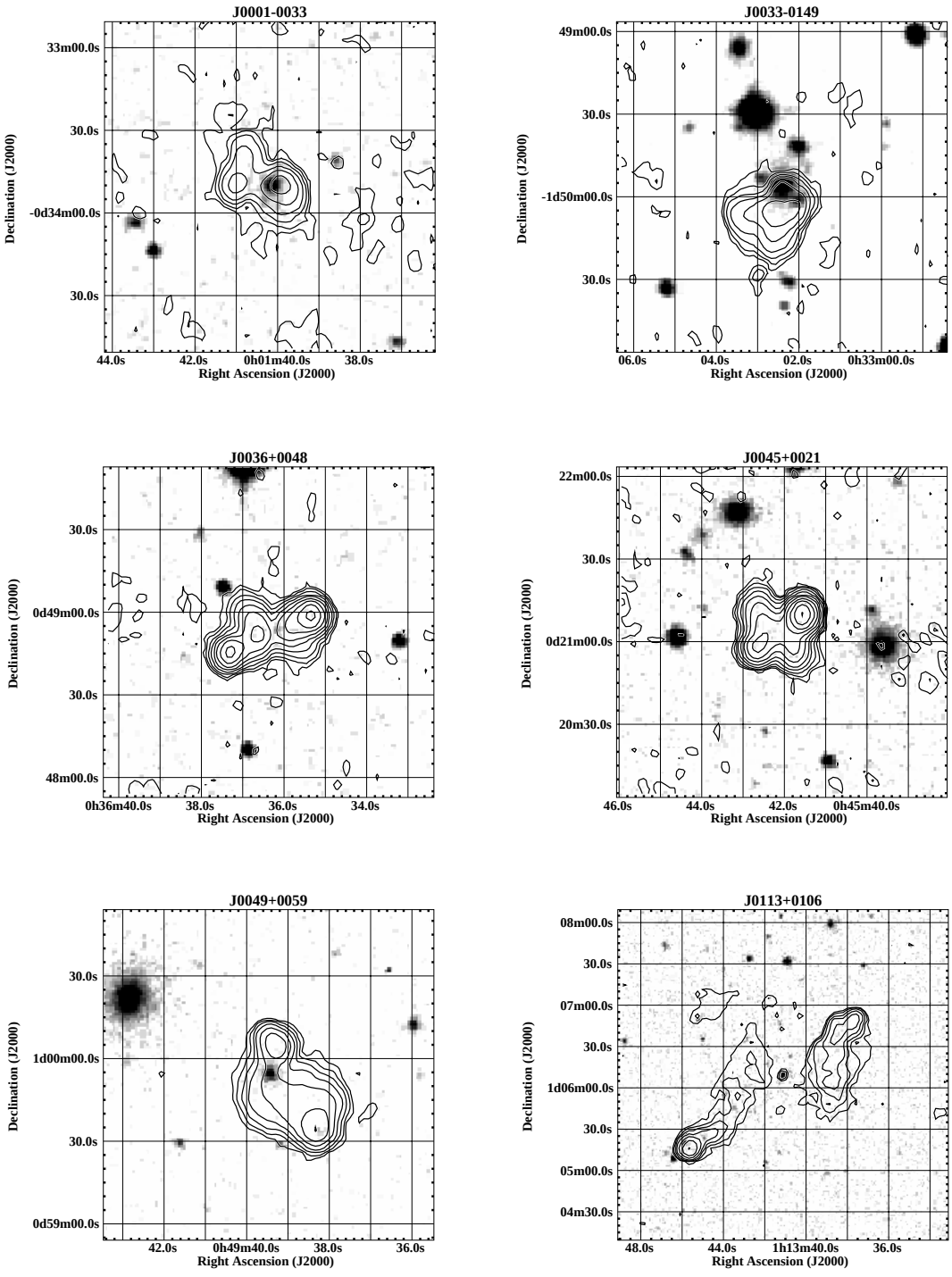

FIG. A4.— VLA-FIRST 1.4 GHz images at 5.4″ resolution (contours) of the 100 candidate X-shaped radio sources overlaid with the DSS2 Red images (greyscale). The fields are centered on the optical counterparts when identified, otherwise, on positions based on the radio morphologies. The lowest radio contour plotted is 0.25 mJy/beam (about 2σ) increasing by factors of two. Image fields are 2×2 arcmin^2 except for the two largest angular size sources, J0113+0106 and J1424+2637, where larger 4×4 arcmin^2 fields are shown.

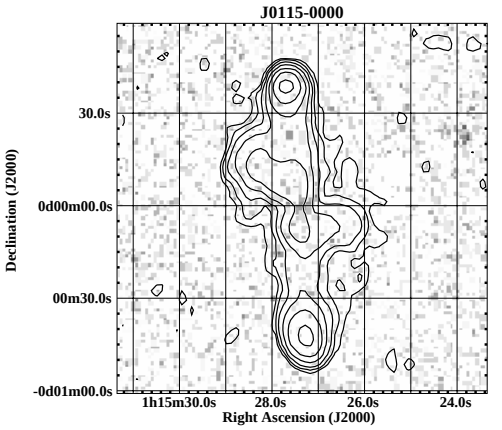
J0115-0000
30.0s
0d00m00.0s
00m30.0s
-0d01m00.0s
Declination (J2000)
1h15m30.0s
28.0s
26.0s
24.0s
Right Ascension (J2000)

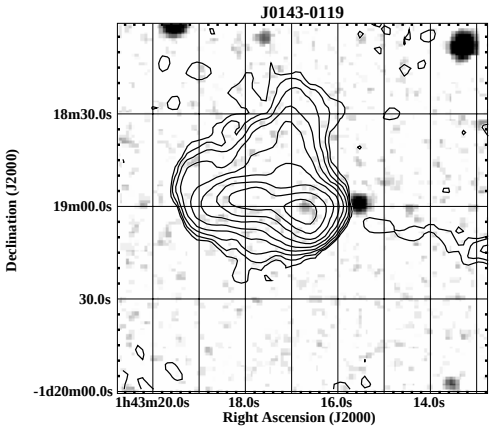
J0143-0119
18m30.0s
19m00.0s
30.0s
-1d20m00.0s
Declination (J2000)
1h43m20.0s
18.0s
16.0s
14.0s
Right Ascension (J2000)

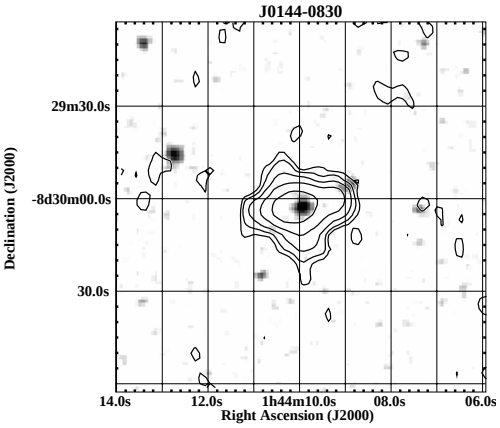
J0144-0830
29m30.0s
-8d30m00.0s
30.0s
Declination (J2000)
14.0s
12.0s
1h44m10.0s
08.0s
06.0s
Right Ascension (J2000)

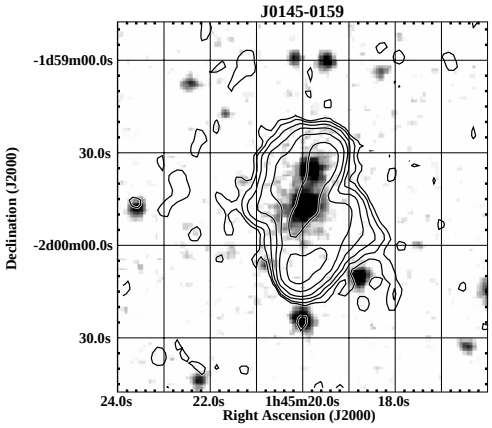
J0145-0159
-1d59m00.0s
30.0s
-2d00m00.0s
30.0s
Declination (J2000)
24.0s
22.0s
1h45m20.0s
18.0s
Right Ascension (J2000)

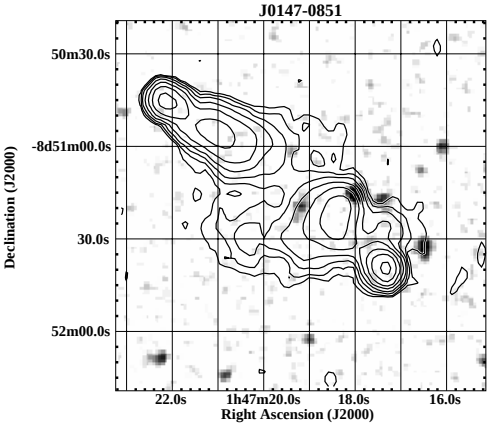
J0147-0851
50m30.0s
-8d51m00.0s
30.0s
52m00.0s
Declination (J2000)
22.0s
1h47m20.0s
18.0s
16.0s
Right Ascension (J2000)

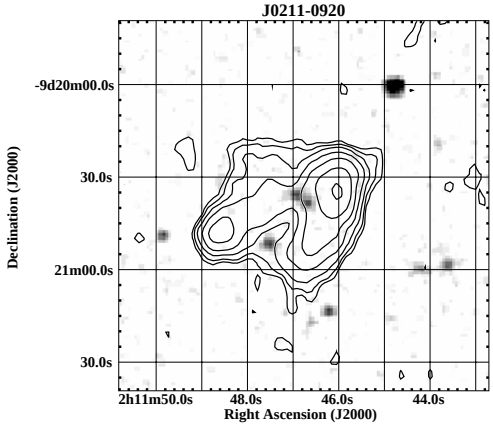
J0211-0920
-9d20m00.0s
30.0s
21m00.0s
30.0s
Declination (J2000)
2h11m50.0s
48.0s
46.0s
44.0s
Right Ascension (J2000)

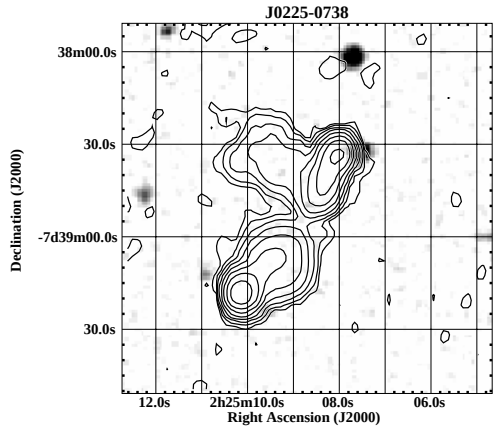
J0225-0738
38m00.0s
30.0s
-7d39m00.0s
30.0s
Declination (J2000)
12.0s
2h25m10.0s
08.0s
06.0s
Right Ascension (J2000)

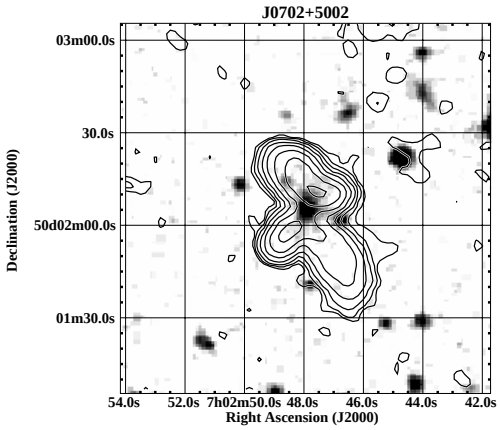
J0702+5002
03m00.0s
30.0s
50d02m00.0s
01m30.0s
Declination (J2000)
54.0s
52.0s
7h02m50.0s
48.0s
46.0s
44.0s
42.0s
Right Ascension (J2000)

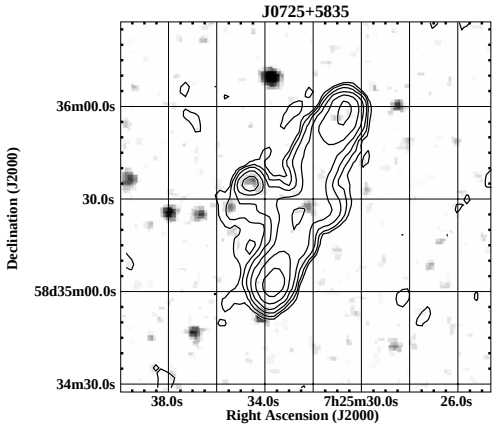
J0725+5835
36m00.0s
30.0s
58d35m00.0s
34m30.0s
Declination (J2000)
38.0s
34.0s
7h25m30.0s
26.0s
Right Ascension (J2000)

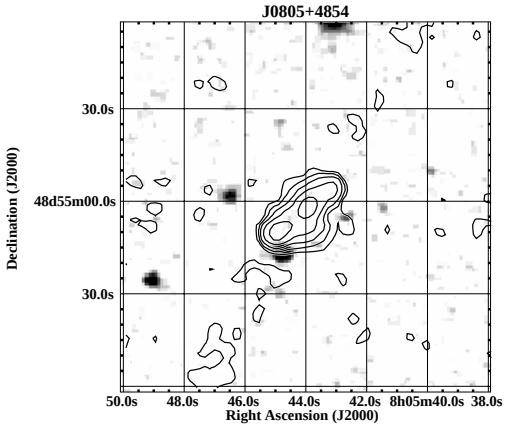
J0805+4854
30.0s
48d55m00.0s
30.0s
Declination (J2000)
50.0s
48.0s
46.0s
44.0s
42.0s
8h05m40.0s
38.0s
Right Ascension (J2000)

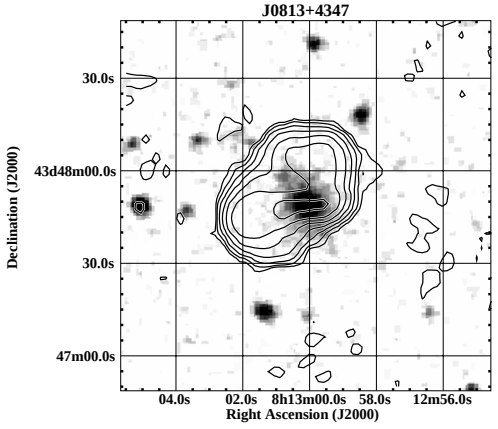
J0813+4347
30.0s
43d48m00.0s
30.0s
47m00.0s
Declination (J2000)
04.0s
02.0s
8h13m00.0s
58.0s
12m56.0s
Right Ascension (J2000)

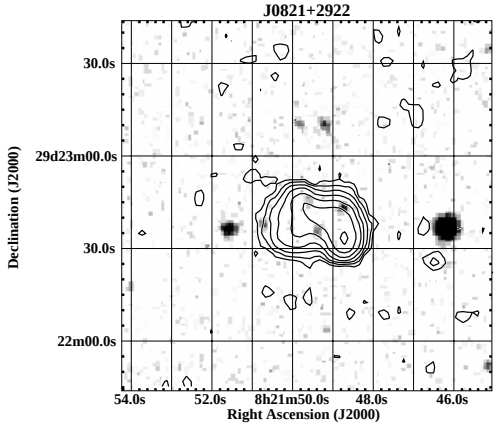
J0821+2922
30.0s
29d23m00.0s
30.0s
22m00.0s
Declination (J2000)
54.0s
52.0s
8h21m50.0s
48.0s
46.0s
Right Ascension (J2000)

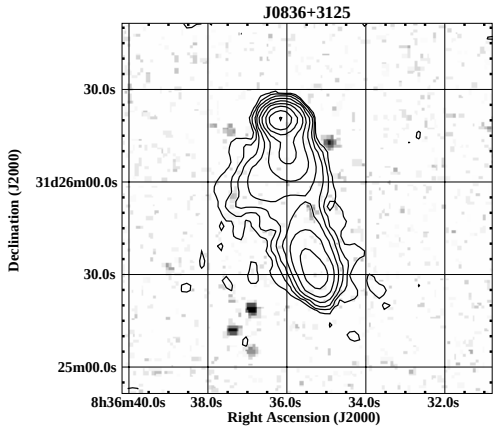
J0836+3125
30.0s
31d26m00.0s
30.0s
25m00.0s
Declination (J2000)
8h36m40.0s
38.0s
36.0s
34.0s
32.0s
Right Ascension (J2000)

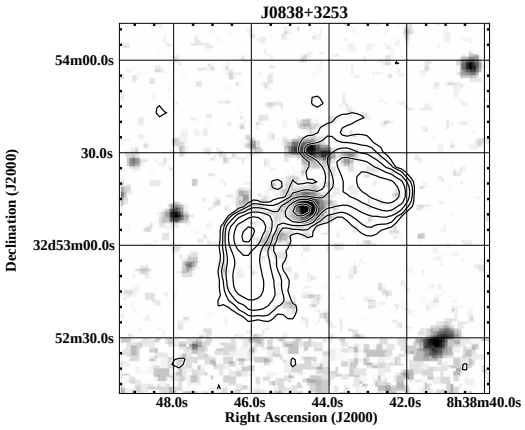
J0838+3253
54m00.0s
30.0s
32d53m00.0s
52m30.0s
Declination (J2000)
48.0s
46.0s
44.0s
42.0s
8h38m40.0s
Right Ascension (J2000)

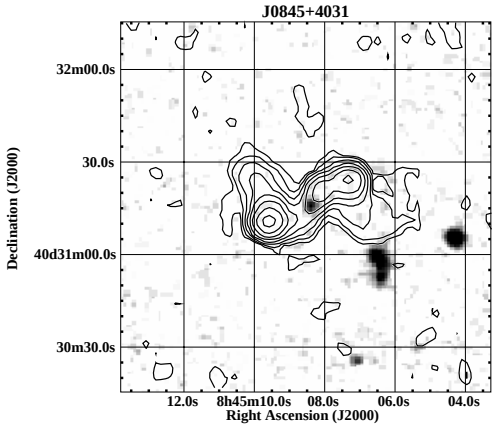
J0845+4031
32m00.0s
30.0s
40d31m00.0s
30m30.0s
Declination (J2000)
12.0s
8h45m10.0s
08.0s
06.0s
04.0s
Right Ascension (J2000)

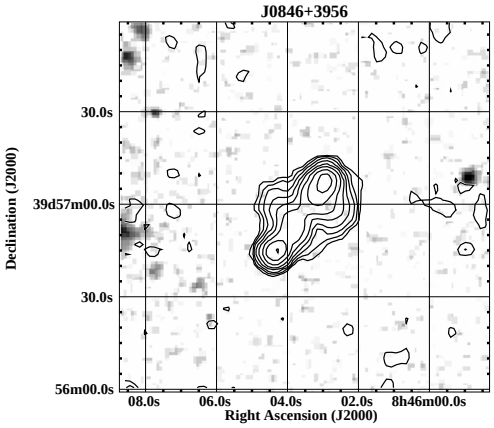
J0846+3956
30.0s
39d57m00.0s
30.0s
56m00.0s
Declination (J2000)
08.0s
06.0s
04.0s
02.0s
8h46m00.0s
Right Ascension (J2000)

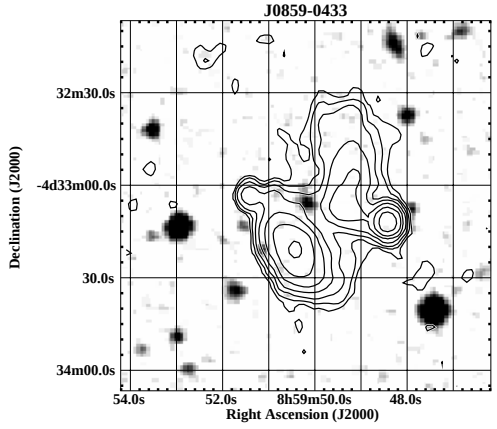
J0859-0433
32m30.0s
-4d33m00.0s
30.0s
34m00.0s
Declination (J2000)
54.0s
52.0s
8h59m50.0s
48.0s
Right Ascension (J2000)

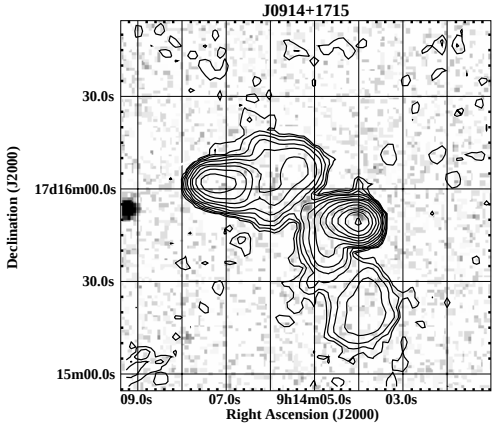
J0914+1715
30.0s
17d16m00.0s
30.0s
15m00.0s
Declination (J2000)
09.0s
07.0s
9h14m05.0s
03.0s
Right Ascension (J2000)

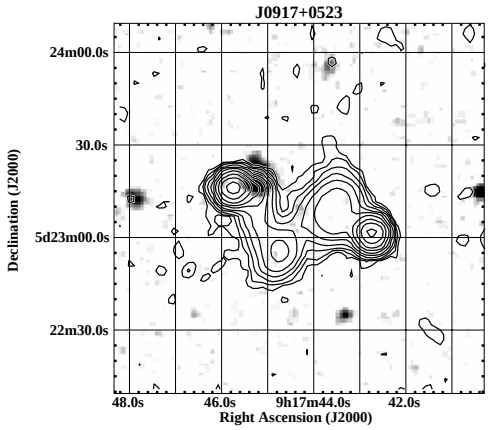
J0917+0523
24m00.0s
30.0s
5d23m00.0s
22m30.0s
Declination (J2000)
48.0s
46.0s
9h17m44.0s
42.0s
Right Ascension (J2000)

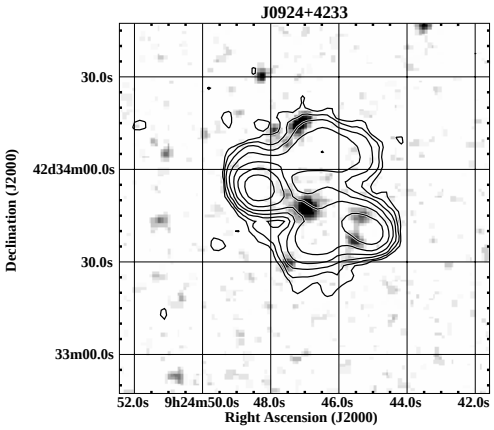
J0924+4233
30.0s
42d34m00.0s
30.0s
33m00.0s
Declination (J2000)
52.0s
9h24m50.0s
48.0s
46.0s
44.0s
42.0s
Right Ascension (J2000)

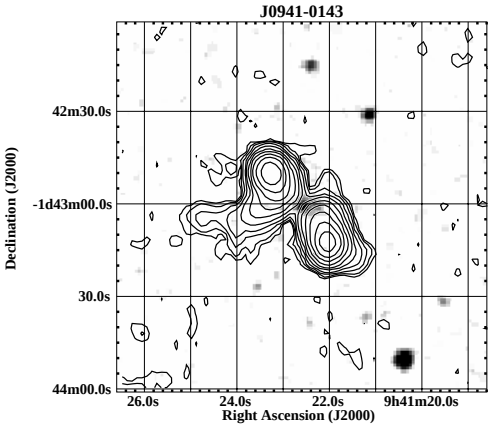
J0941-0143
42m30.0s
-1d43m00.0s
30.0s
44m00.0s
Declination (J2000)
26.0s
24.0s
22.0s
9h41m20.0s
Right Ascension (J2000)

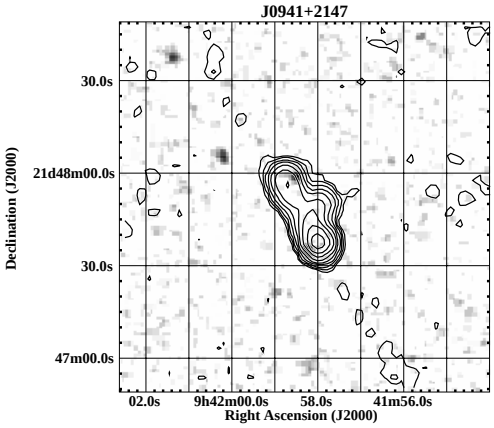
J0941+2147
30.0s
21d48m00.0s
30.0s
47m00.0s
Declination (J2000)
02.0s
9h42m00.0s
58.0s
41m56.0s
Right Ascension (J2000)

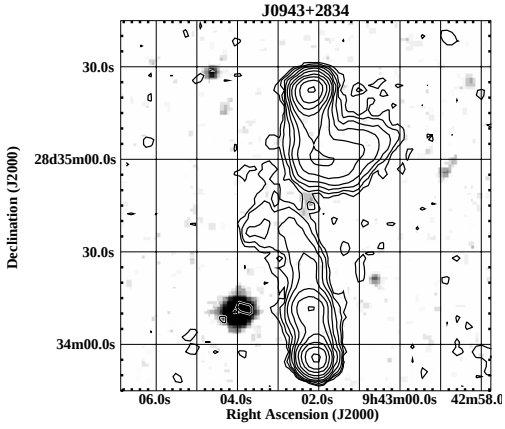
J0943+2834
30.0s
28d35m00.0s
30.0s
34m00.0s
Declination (J2000)
06.0s
04.0s
02.0s
9h43m00.0s
Right Ascension (J2000)

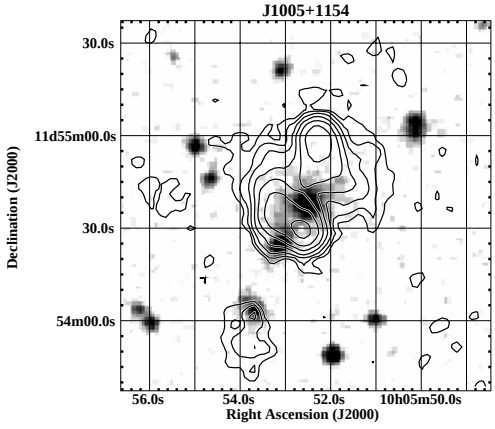
J1005+1154
30.0s
11d55m00.0s
30.0s
54m00.0s
Declination (J2000)
56.0s
54.0s
52.0s
10h05m50.0s
Right Ascension (J2000)

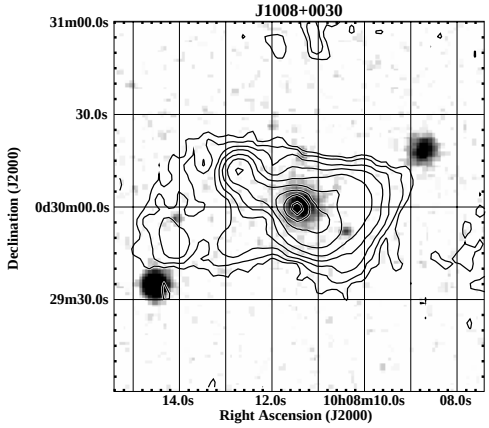
J1008+0030
31m00.0s
30.0s
0d30m00.0s
29m30.0s
Declination (J2000)
14.0s
12.0s
10h08m10.0s
08.0s
Right Ascension (J2000)

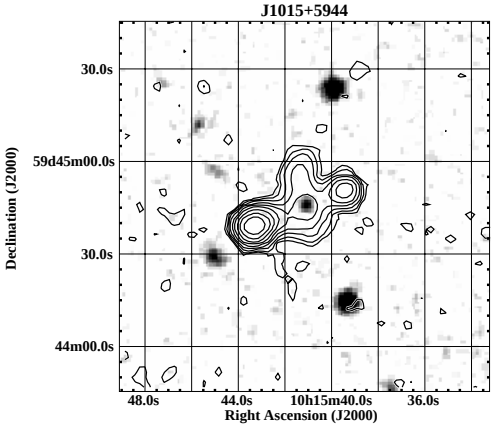
J1015+5944
30.0s
59d45m00.0s
30.0s
44m00.0s
Declination (J2000)
48.0s
44.0s
10h15m40.0s
36.0s
Right Ascension (J2000)

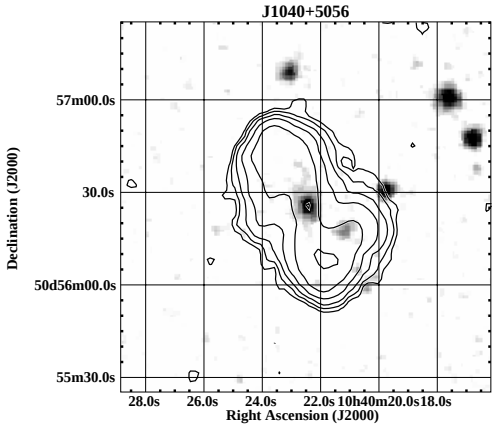
J1040+5056
57m00.0s
30.0s
50d56m00.0s
55m30.0s
Declination (J2000)
28.0s
26.0s
24.0s
22.0s
10h40m20.0s
18.0s
Right Ascension (J2000)

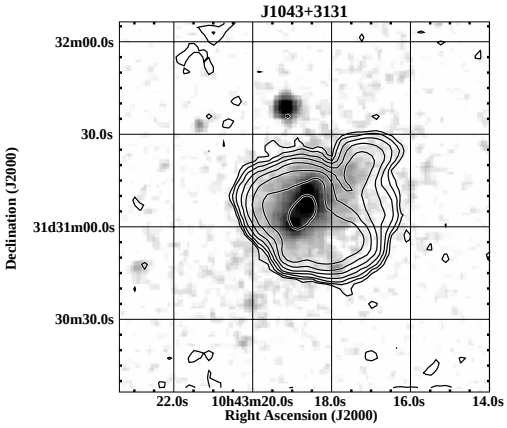
J1043+3131
32m00.0s
30.0s
31d31m00.0s
30m30.0s
Declination (J2000)
22.0s
10h43m20.0s
18.0s
16.0s
14.0s
Right Ascension (J2000)

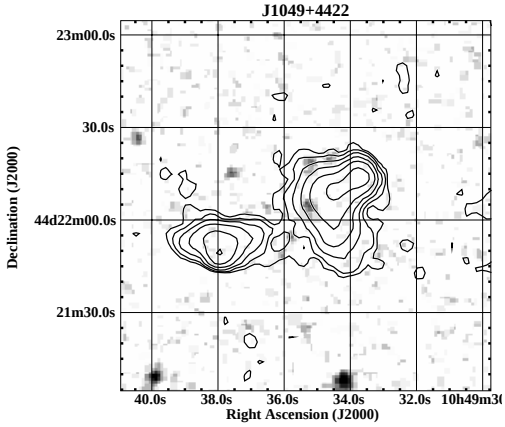
J1049+4422
23m00.0s
30.0s
44d22m00.0s
21m30.0s
Declination (J2000)
40.0s
38.0s
36.0s
34.0s
32.0s
Right Ascension (J2000)

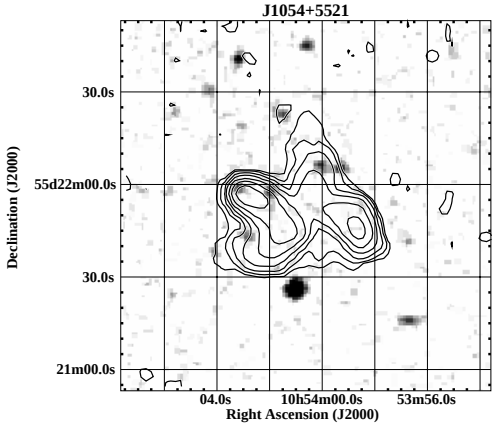
J1054+5521
30.0s
55d22m00.0s
30.0s
21m00.0s
Declination (J2000)
04.0s
10h54m00.0s
53m56.0s
Right Ascension (J2000)

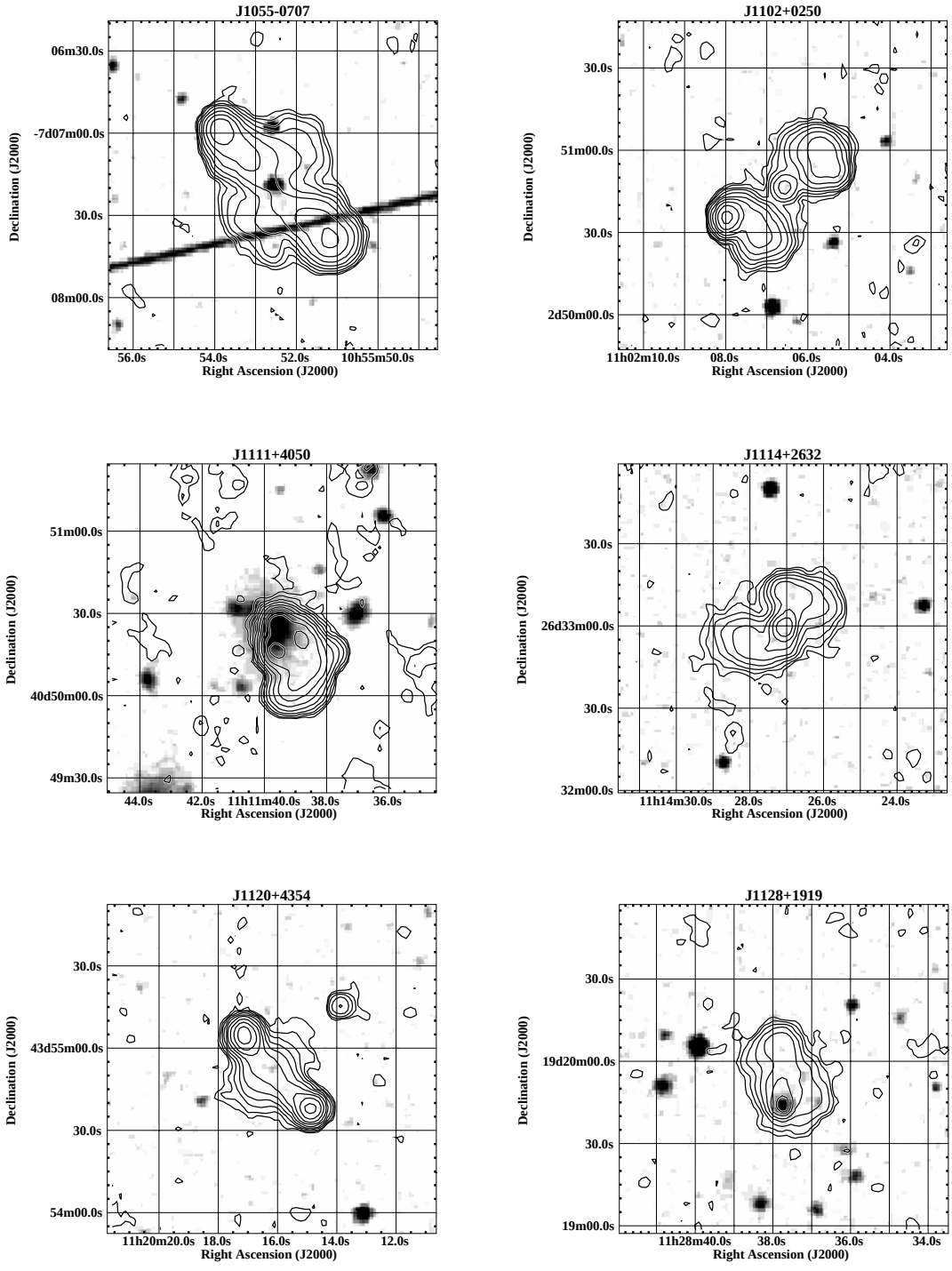
J1055-0707
06m30.0s
-7d07m00.0s
30.0s
08m00.0s
Declination (J2000)
56.0s
54.0s
52.0s
10h55m50.0s
Right Ascension (J2000)
J1102+0250
30.0s
51m00.0s
30.0s
2d50m00.0s
Declination (J2000)
11h02m10.0s
08.0s
06.0s
04.0s
Right Ascension (J2000)
J1111+4050
51m00.0s
30.0s
40d50m00.0s
49m30.0s
Declination (J2000)
44.0s
42.0s
11h11m40.0s
38.0s
36.0s
Right Ascension (J2000)
J1114+2632
30.0s
26d33m00.0s
30.0s
32m00.0s
Declination (J2000)
11h14m30.0s
28.0s
26.0s
24.0s
Right Ascension (J2000)
J1120+4354
30.0s
43d55m00.0s
30.0s
54m00.0s
Declination (J2000)
11h20m20.0s
18.0s
16.0s
14.0s
12.0s
Right Ascension (J2000)
J1128+1919
30.0s
19d20m00.0s
30.0s
19m00.0s
Declination (J2000)
11h28m40.0s
38.0s
36.0s
34.0s
Right Ascension (J2000)

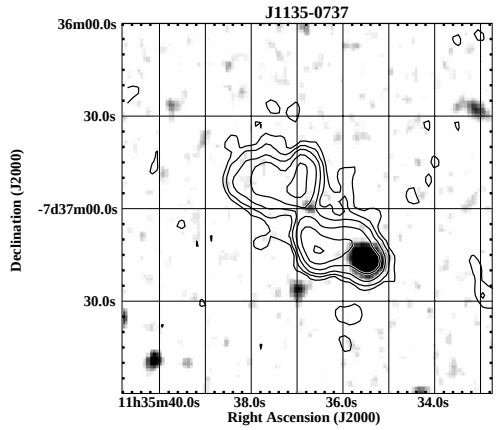
J1135-0737
36m00.0s
30.0s
-7d37m00.0s
30.0s
Declination (J2000)
11h35m40.0s
38.0s
36.0s
34.0s
Right Ascension (J2000)

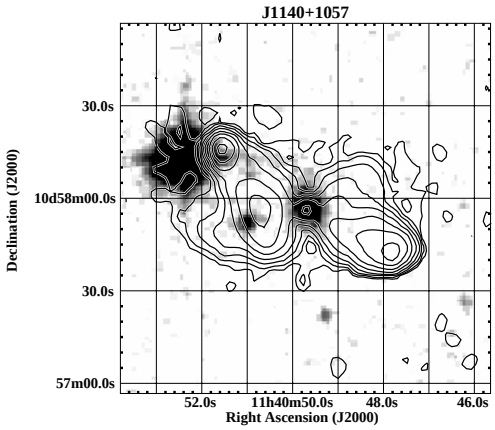
J1140+1057
30.0s
10d58m00.0s
30.0s
57m00.0s
Declination (J2000)
52.0s
11h40m50.0s
48.0s
46.0s
Right Ascension (J2000)

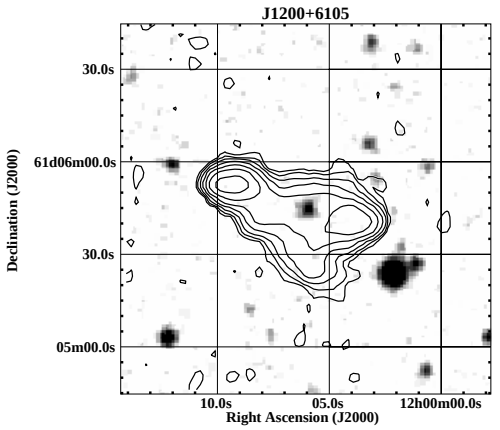
J1200+6105
30.0s
61d06m00.0s
30.0s
05m00.0s
Declination (J2000)
10.0s
05.0s
12h00m00.0s
Right Ascension (J2000)

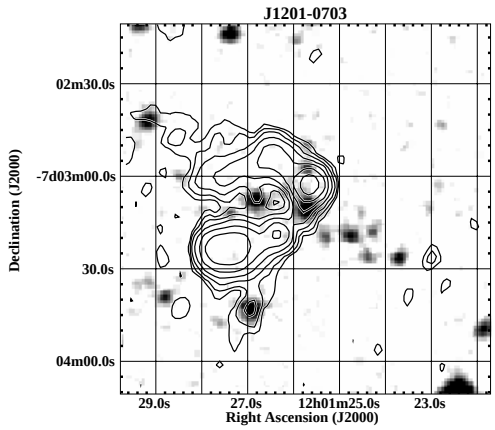
J1201-0703
02m30.0s
-7d03m00.0s
30.0s
04m00.0s
Declination (J2000)
29.0s
27.0s
12h01m25.0s
23.0s
Right Ascension (J2000)

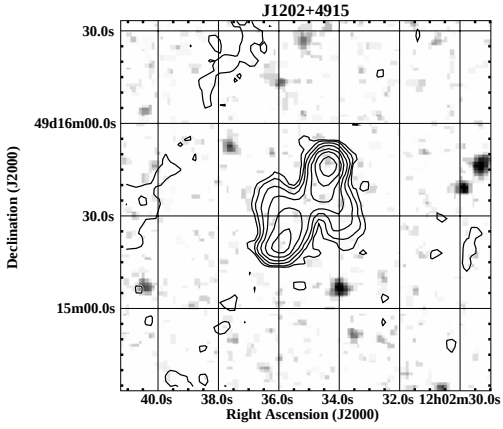
J1202+4915
30.0s
49d16m00.0s
30.0s
15m00.0s
Declination (J2000)
40.0s
38.0s
36.0s
34.0s
32.0s
12h02m30.0s
Right Ascension (J2000)

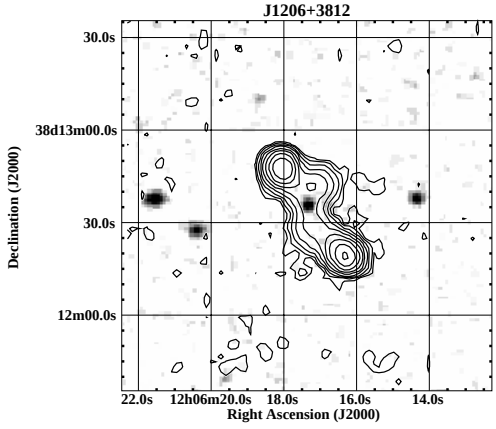
J1206+3812
30.0s
38d13m00.0s
30.0s
12m00.0s
Declination (J2000)
22.0s
12h06m20.0s
18.0s
16.0s
14.0s
Right Ascension (J2000)

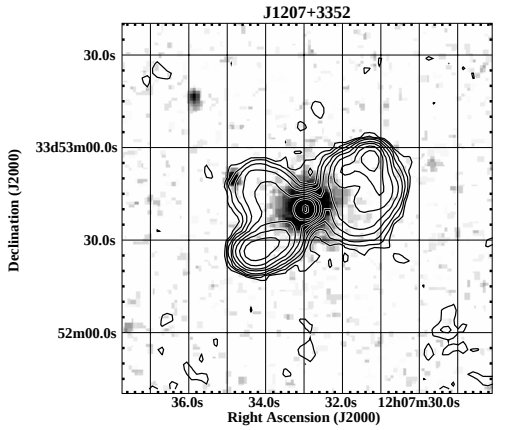
J1207+3352
30.0s
33d53m00.0s
30.0s
52m00.0s
Declination (J2000)
36.0s
34.0s
32.0s
12h07m30.0s
Right Ascension (J2000)

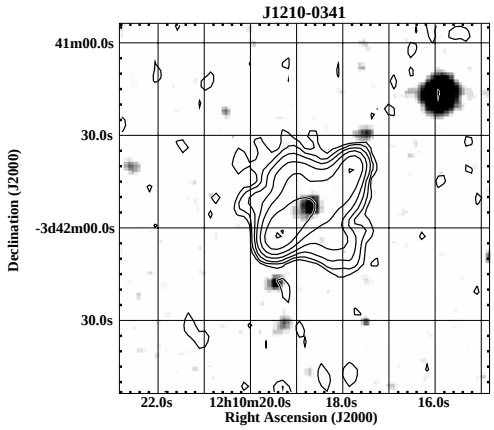
J1210-0341
41m00.0s
30.0s
-3d42m00.0s
30.0s
Declination (J2000)
22.0s
12h10m20.0s
18.0s
16.0s
Right Ascension (J2000)

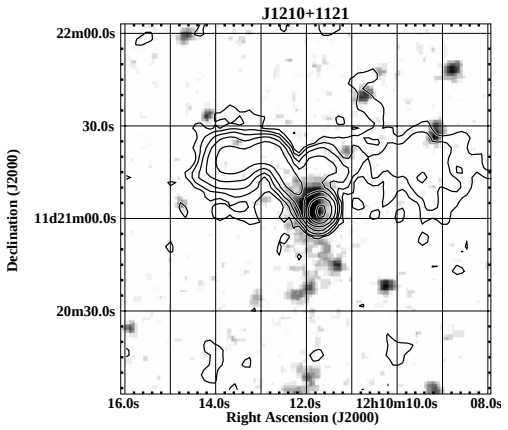
J1210+1121
22m00.0s
30.0s
11d21m00.0s
20m30.0s
Declination (J2000)
16.0s
14.0s
12.0s
12h10m10.0s
08.0s
Right Ascension (J2000)

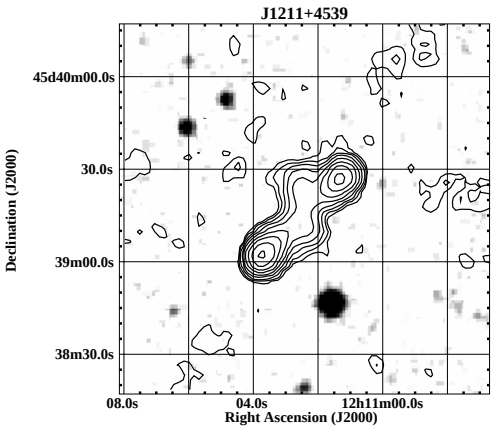
J1211+4539
45d40m00.0s
30.0s
39m00.0s
38m30.0s
Declination (J2000)
08.0s
04.0s
12h11m00.0s
Right Ascension (J2000)

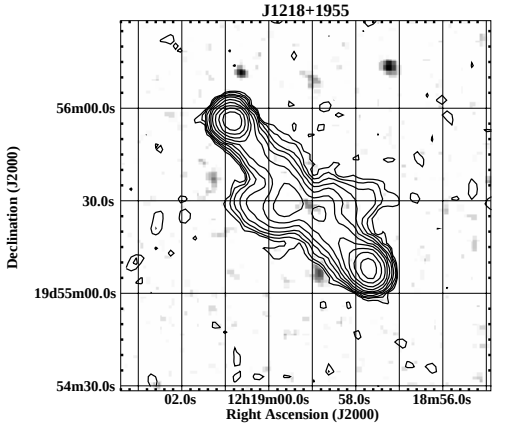
J1218+1955
56m00.0s
30.0s
19d55m00.0s
54m30.0s
Declination (J2000)
02.0s
12h19m00.0s
58.0s
18m56.0s
Right Ascension (J2000)

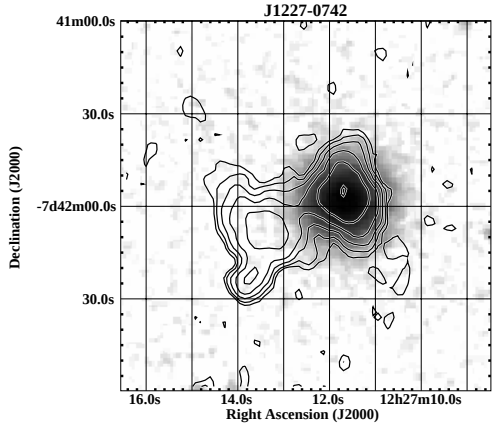
J1227-0742
41m00.0s
30.0s
-7d42m00.0s
30.0s
Declination (J2000)
16.0s
14.0s
12.0s
12h27m10.0s
Right Ascension (J2000)

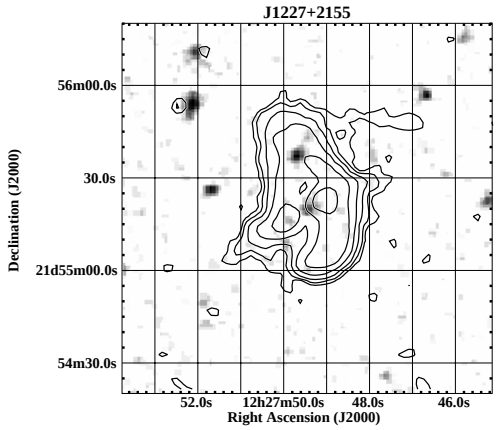
J1227+2155
56m00.0s
30.0s
21d55m00.0s
54m30.0s
Declination (J2000)
52.0s
12h27m50.0s
48.0s
46.0s
Right Ascension (J2000)

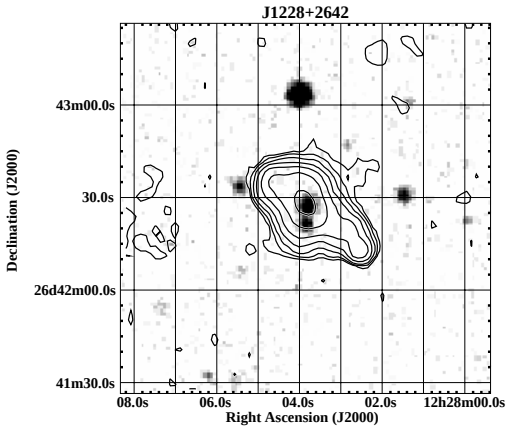
J1228+2642
43m00.0s
30.0s
26d42m00.0s
41m30.0s
Declination (J2000)
08.0s
06.0s
04.0s
02.0s
12h28m00.0s
Right Ascension (J2000)

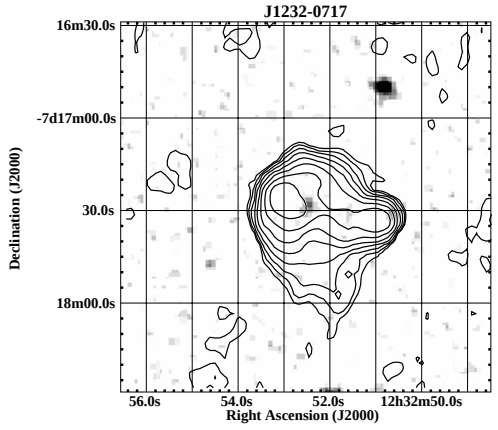
J1232-0717
16m30.0s
-7d17m00.0s
30.0s
18m00.0s
Declination (J2000)
56.0s
54.0s
52.0s
12h32m50.0s
Right Ascension (J2000)

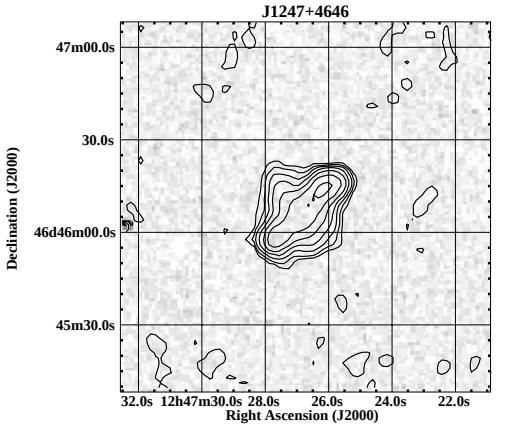
J1247+4646
47m00.0s
30.0s
46d46m00.0s
45m30.0s
Declination (J2000)
32.0s
12h47m30.0s
28.0s
26.0s
24.0s
22.0s
Right Ascension (J2000)

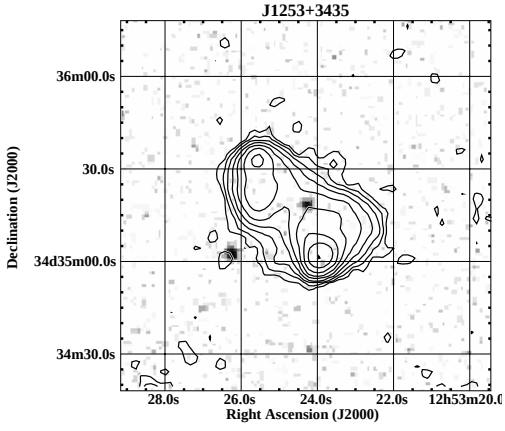
J1253+3435
36m00.0s
30.0s
34d35m00.0s
34m30.0s
Declination (J2000)
28.0s
26.0s
24.0s
22.0s
Right Ascension (J2000)

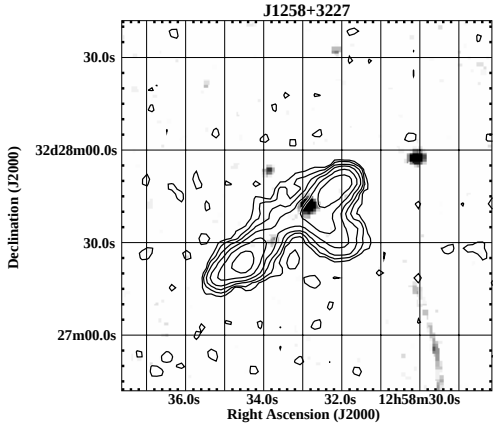
J1258+3227
30.0s
32d28m00.0s
30.0s
27m00.0s
Declination (J2000)
36.0s
34.0s
32.0s
12h58m30.0s
Right Ascension (J2000)

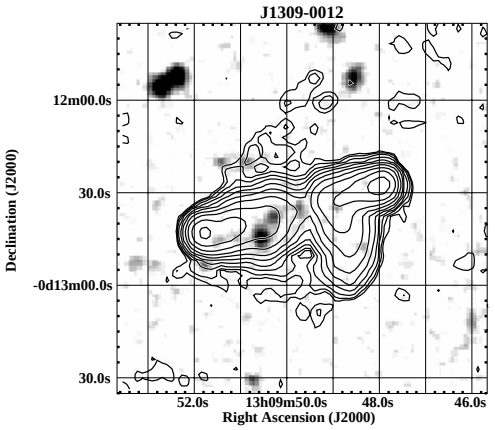
J1309-0012
12m00.0s
30.0s
-0d13m00.0s
30.0s
Declination (J2000)
52.0s
13h09m50.0s
48.0s
46.0s
Right Ascension (J2000)

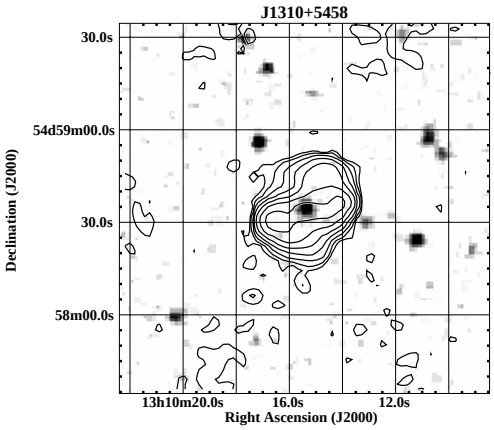
J1310+5458
30.0s
54d59m00.0s
30.0s
58m00.0s
Declination (J2000)
13h10m20.0s
16.0s
12.0s
Right Ascension (J2000)

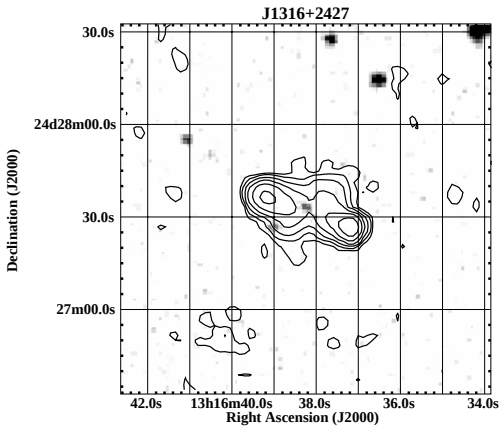
J1316+2427
30.0s
24d28m00.0s
30.0s
27m00.0s
Declination (J2000)
42.0s
13h16m40.0s
38.0s
36.0s
34.0s
Right Ascension (J2000)

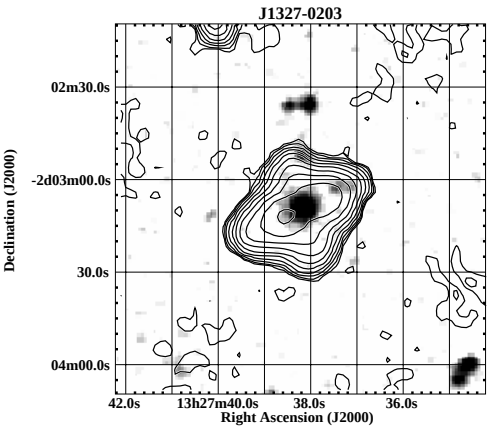
J1327-0203
02m30.0s
-2d03m00.0s
30.0s
04m00.0s
Declination (J2000)
42.0s
13h27m40.0s
38.0s
36.0s
Right Ascension (J2000)

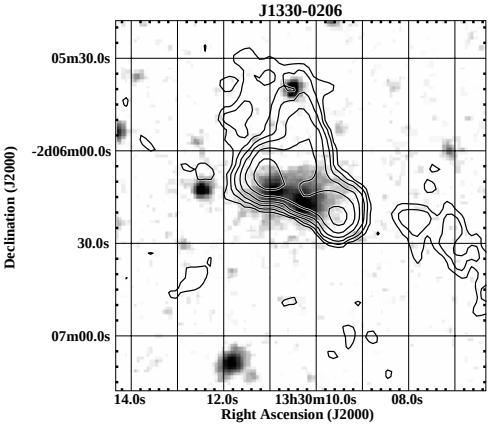
J1330-0206
05m30.0s
-2d06m00.0s
30.0s
07m00.0s
Declination (J2000)
14.0s
12.0s
13h30m10.0s
08.0s
Right Ascension (J2000)

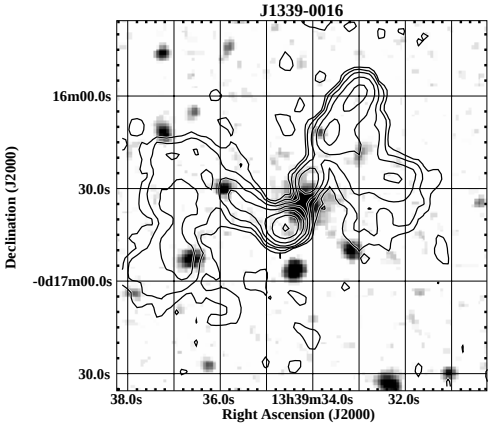
J1339-0016
16m00.0s
30.0s
-0d17m00.0s
30.0s
Declination (J2000)
38.0s
36.0s
13h39m34.0s
32.0s
Right Ascension (J2000)

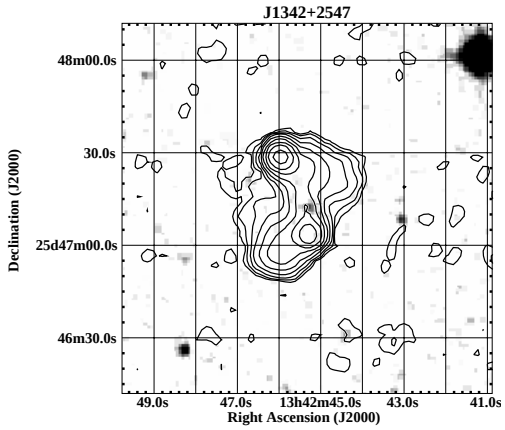
J1342+2547
48m00.0s
30.0s
25d47m00.0s
46m30.0s
Declination (J2000)
49.0s
47.0s
13h42m45.0s
43.0s
41.0s
Right Ascension (J2000)

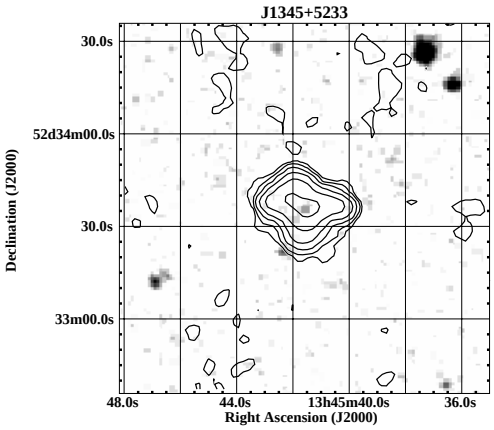
J1345+5233
30.0s
52d34m00.0s
30.0s
33m00.0s
Declination (J2000)
48.0s
44.0s
13h45m40.0s
36.0s
Right Ascension (J2000)

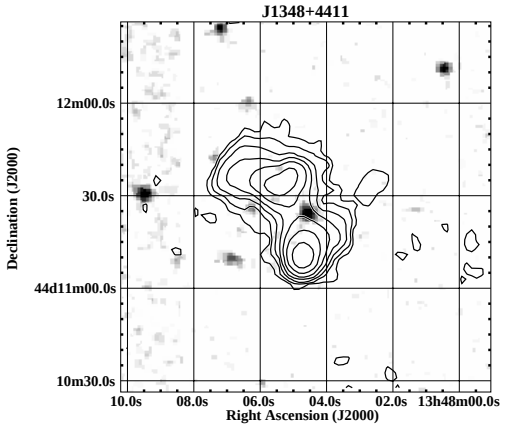
J1348+4411
12m00.0s
30.0s
44d11m00.0s
10m30.0s
Declination (J2000)
10.0s
08.0s
06.0s
04.0s
02.0s
13h48m00.0s
Right Ascension (J2000)

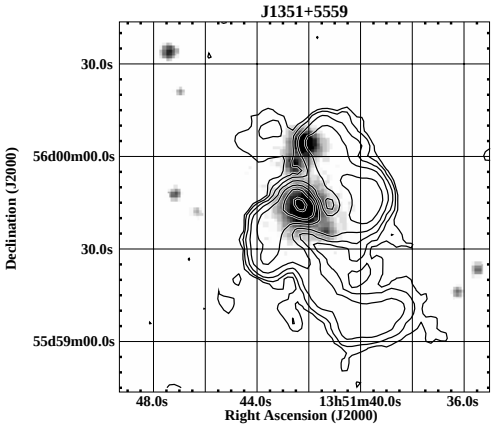
J1351+5559
30.0s
56d00m00.0s
30.0s
55d59m00.0s
Declination (J2000)
48.0s
44.0s
13h51m40.0s
36.0s
Right Ascension (J2000)

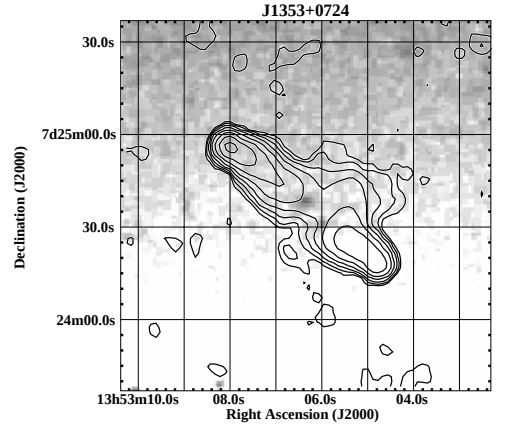
J1353+0724
30.0s
7d25m00.0s
30.0s
24m00.0s
Declination (J2000)
13h53m10.0s
08.0s
06.0s
04.0s
Right Ascension (J2000)

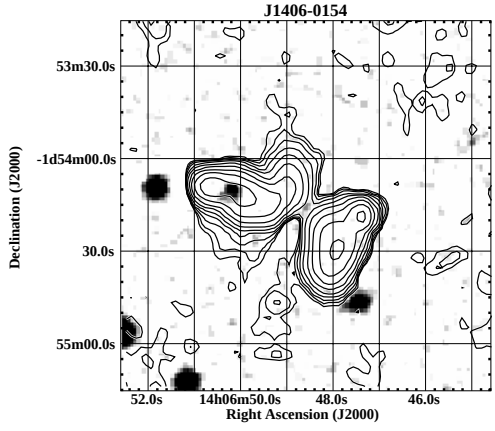
J1406-0154
53m30.0s
-1d54m00.0s
30.0s
55m00.0s
Declination (J2000)
52.0s
14h06m50.0s
48.0s
46.0s
Right Ascension (J2000)

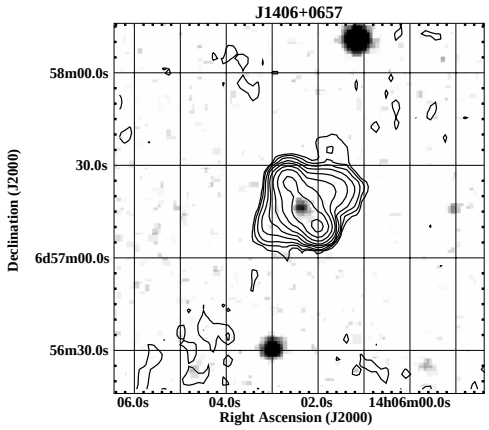
J1406+0657
58m00.0s
30.0s
6d57m00.0s
56m30.0s
Declination (J2000)
06.0s
04.0s
02.0s
14h06m00.0s
Right Ascension (J2000)

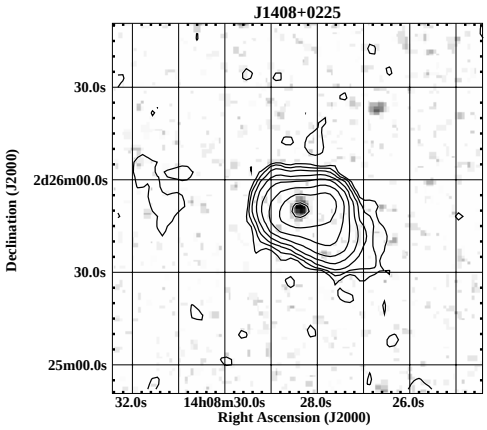
J1408+0225
30.0s
2d26m00.0s
30.0s
25m00.0s
Declination (J2000)
32.0s
14h08m30.0s
28.0s
26.0s
Right Ascension (J2000)

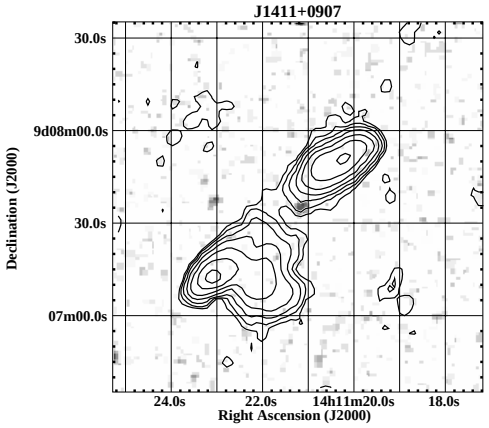
J1411+0907
30.0s
9d08m00.0s
30.0s
07m00.0s
Declination (J2000)
24.0s
22.0s
14h11m20.0s
18.0s
Right Ascension (J2000)

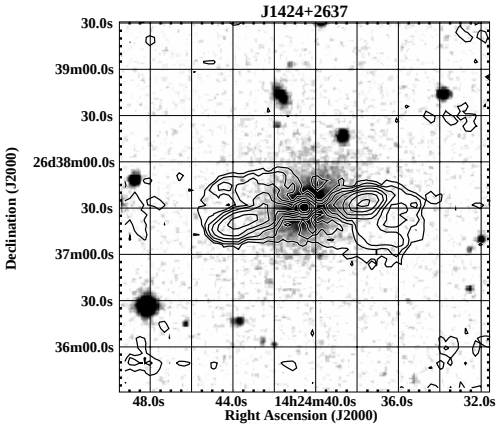
J1424+2637
30.0s
39m00.0s
30.0s
26d38m00.0s
30.0s
37m00.0s
30.0s
36m00.0s
Declination (J2000)
48.0s
44.0s
14h24m40.0s
36.0s
32.0s
Right Ascension (J2000)

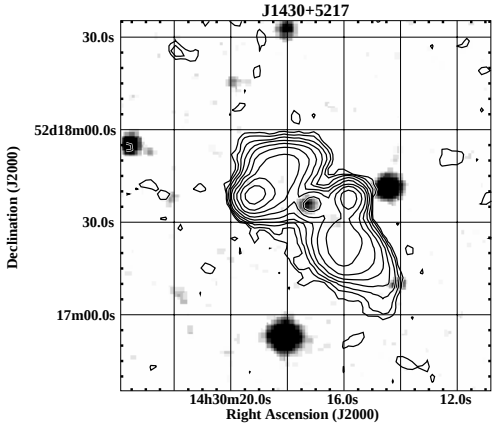
J1430+5217
30.0s
52d18m00.0s
30.0s
17m00.0s
Declination (J2000)
14h30m20.0s
16.0s
12.0s
Right Ascension (J2000)

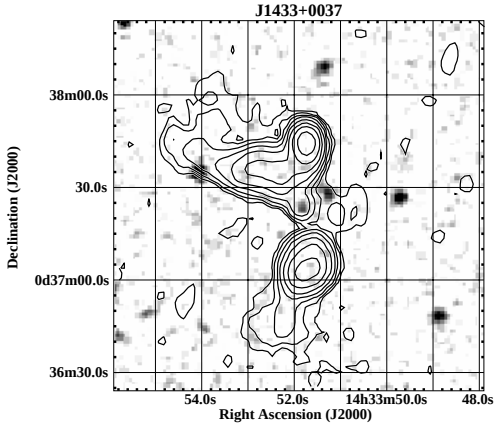
J1433+0037
38m00.0s
30.0s
0d37m00.0s
36m30.0s
Declination (J2000)
54.0s
52.0s
14h33m50.0s
48.0s
Right Ascension (J2000)

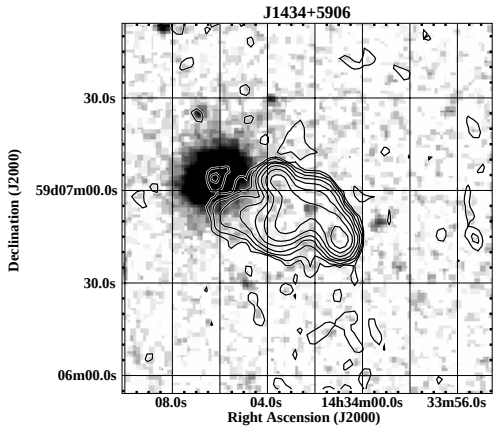
J1434+5906
30.0s
59d07m00.0s
30.0s
06m00.0s
Declination (J2000)
08.0s
04.0s
14h34m00.0s
33m56.0s
Right Ascension (J2000)

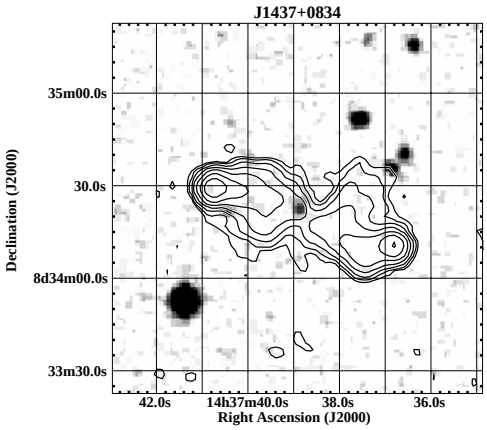
J1437+0834
35m00.0s
30.0s
8d34m00.0s
33m30.0s
Declination (J2000)
42.0s
14h37m40.0s
38.0s
36.0s
Right Ascension (J2000)

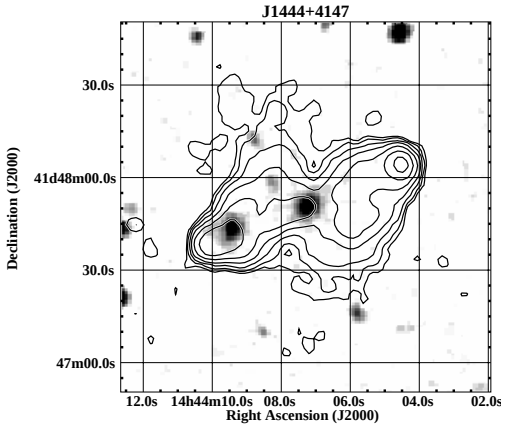
J1444+4147
30.0s
41d48m00.0s
30.0s
47m00.0s
Declination (J2000)
12.0s
14h44m10.0s
08.0s
06.0s
04.0s
02.0s
Right Ascension (J2000)

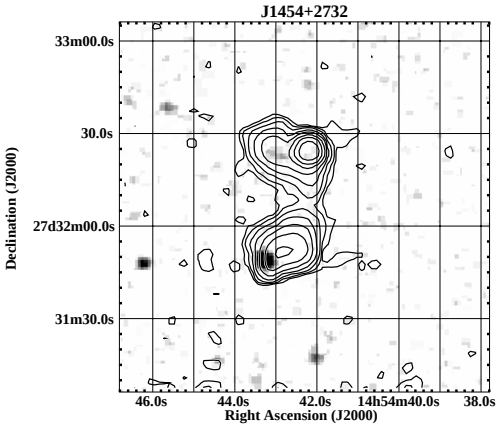
J1454+2732
33m00.0s
30.0s
27d32m00.0s
31m30.0s
Declination (J2000)
46.0s
44.0s
42.0s
14h54m40.0s
38.0s
Right Ascension (J2000)

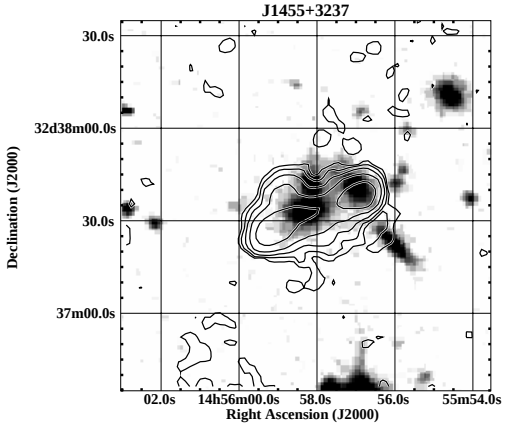
J1455+3237
30.0s
32d38m00.0s
30.0s
37m00.0s
Declination (J2000)
02.0s
14h56m00.0s
58.0s
56.0s
55m54.0s
Right Ascension (J2000)

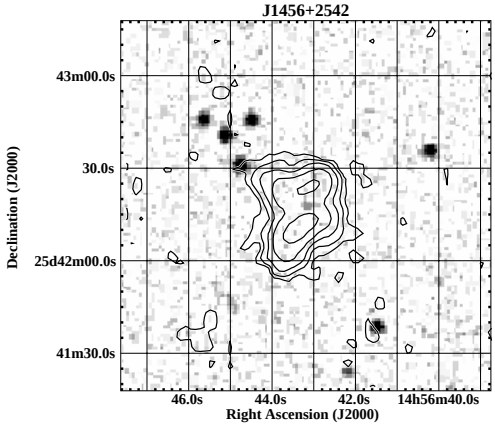
J1456+2542
43m00.0s
30.0s
25d42m00.0s
41m30.0s
Declination (J2000)
46.0s
44.0s
42.0s
14h56m40.0s
Right Ascension (J2000)

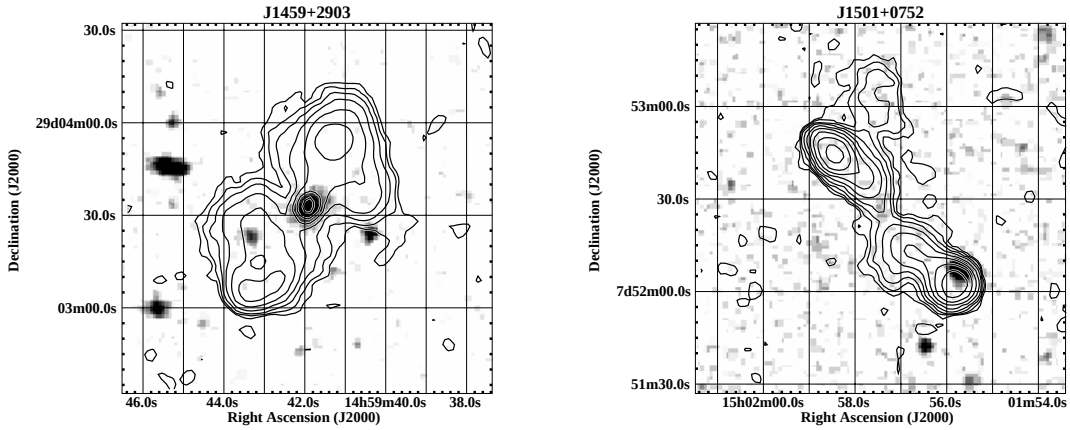
J1459+2903
30.0s
29d04m00.0s
30.0s
03m00.0s
Declination (J2000)
46.0s
44.0s
42.0s
14h59m40.0s
38.0s
Right Ascension (J2000)

J1501+0752
53m00.0s
30.0s
7d52m00.0s
51m30.0s
Declination (J2000)
15h02m00.0s
58.0s
56.0s
01m54.0s
Right Ascension (J2000)

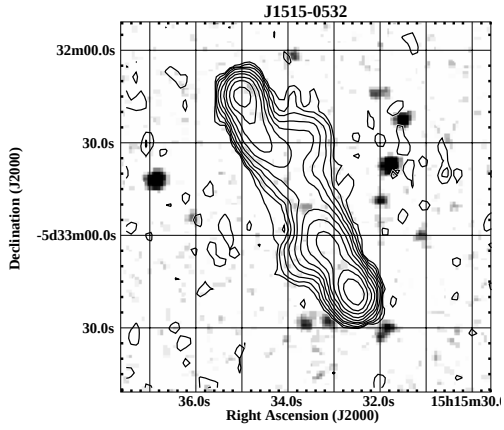
J1515-0532
32m00.0s
30.0s
-5d33m00.0s
30.0s
Declination (J2000)
36.0s
34.0s
32.0s
15h15m30.
Right Ascension (J2000)

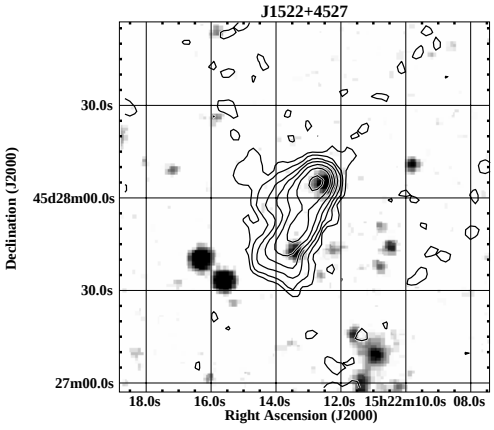
J1522+4527
30.0s
45d28m00.0s
30.0s
27m00.0s
Declination (J2000)
18.0s
16.0s
14.0s
12.0s
15h22m10.0s
08.0s
Right Ascension (J2000)

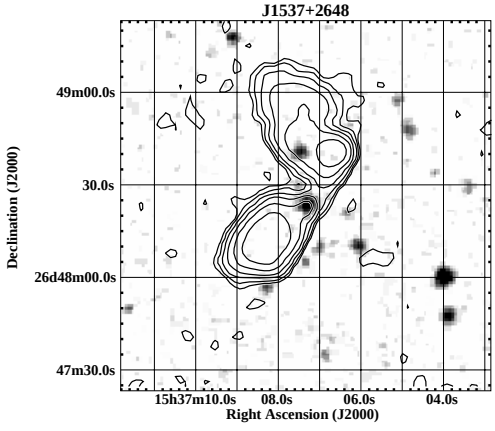
J1537+2648
49m00.0s
30.0s
26d48m00.0s
47m30.0s
Declination (J2000)
15h37m10.0s
08.0s
06.0s
04.0s
Right Ascension (J2000)

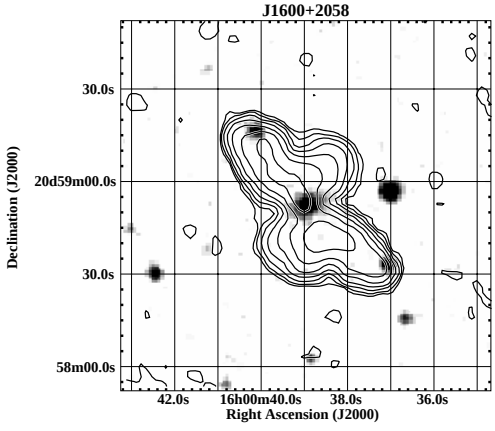
J1600+2058
30.0s
20d59m00.0s
30.0s
58m00.0s
Declination (J2000)
42.0s
16h00m40.0s
38.0s
36.0s
Right Ascension (J2000)

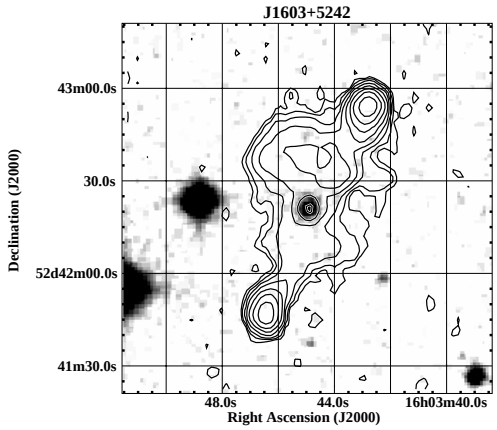
J1603+5242
43m00.0s
30.0s
52d42m00.0s
41m30.0s
Declination (J2000)
48.0s
44.0s
16h03m40.0s
Right Ascension (J2000)

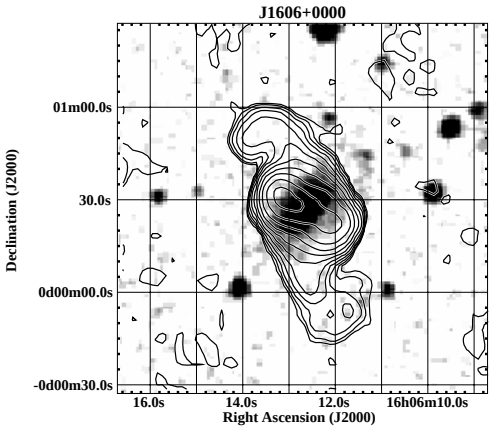
J1606+0000
01m00.0s
30.0s
0d00m00.0s
-0d00m30.0s
Declination (J2000)
16.0s
14.0s
12.0s
16h06m10.0s
Right Ascension (J2000)

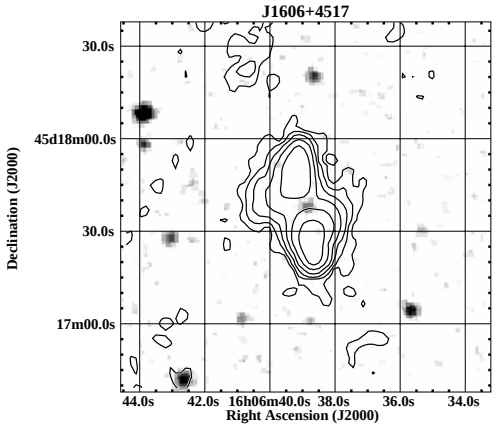
J1606+4517
30.0s
45d18m00.0s
30.0s
17m00.0s
Declination (J2000)
44.0s
42.0s
16h06m40.0s
38.0s
36.0s
34.0s
Right Ascension (J2000)

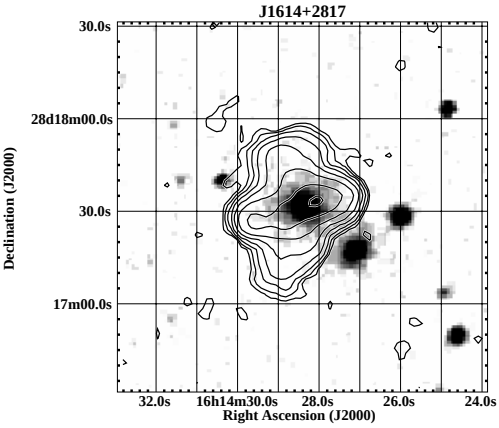
J1614+2817
30.0s
28d18m00.0s
30.0s
17m00.0s
Declination (J2000)
32.0s
16h14m30.0s
28.0s
26.0s
24.0s
Right Ascension (J2000)

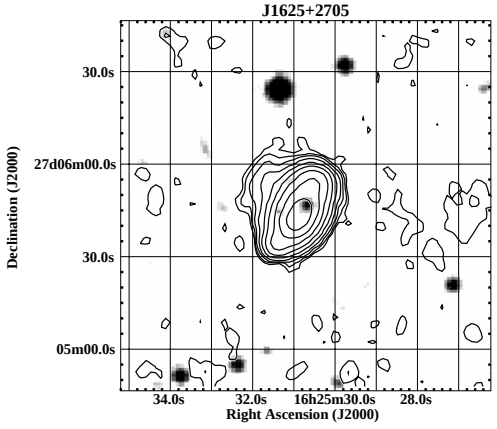
J1625+2705
30.0s
27d06m00.0s
30.0s
05m00.0s
Declination (J2000)
34.0s
32.0s
16h25m30.0s
28.0s
Right Ascension (J2000)

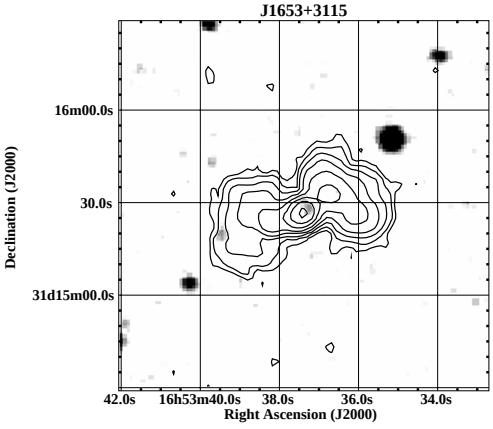
J1653+3115
16m00.0s
30.0s
31d15m00.0s
Declination (J2000)
42.0s
16h53m40.0s
38.0s
36.0s
34.0s
Right Ascension (J2000)

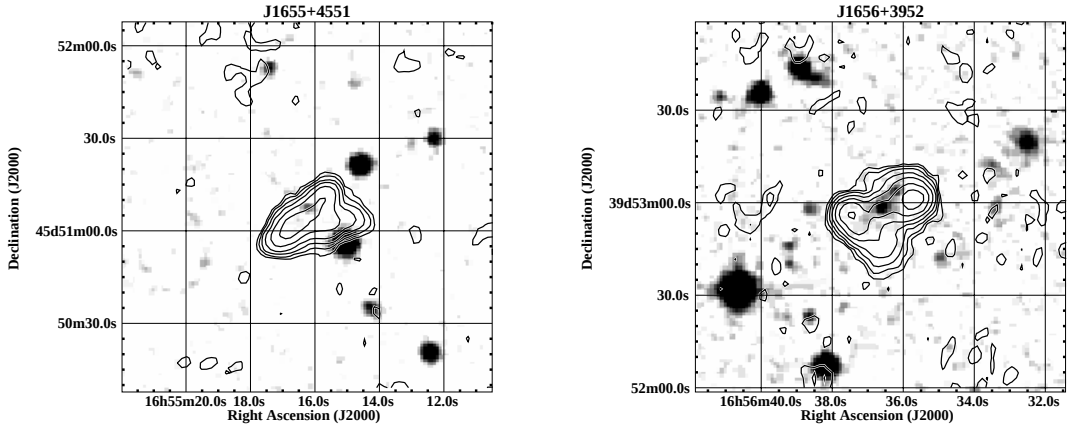
J1655+4551
52m00.0s
30.0s
45d51m00.0s
50m30.0s
Declination (J2000)
16h55m20.0s
18.0s
16.0s
14.0s
12.0s
Right Ascension (J2000)
J1656+3952
30.0s
39d53m00.0s
30.0s
52m00.0s
Declination (J2000)
16h56m40.0s
38.0s
36.0s
34.0s
32.0s
Right Ascension (J2000)
J2226+0125
26m00.0s
30.0s
1d25m00.0s
24m30.0s
Declination (J2000)
49.0s
47.0s
22h26m45.0s
43.0s
Right Ascension (J2000)
J2359-1041
40m30.0s
-10d41m00.0s
30.0s
42m00.0s
Declination (J2000)
23h59m50.0s
48.0s
46.0s
44.0s
Right Ascension (J2000)

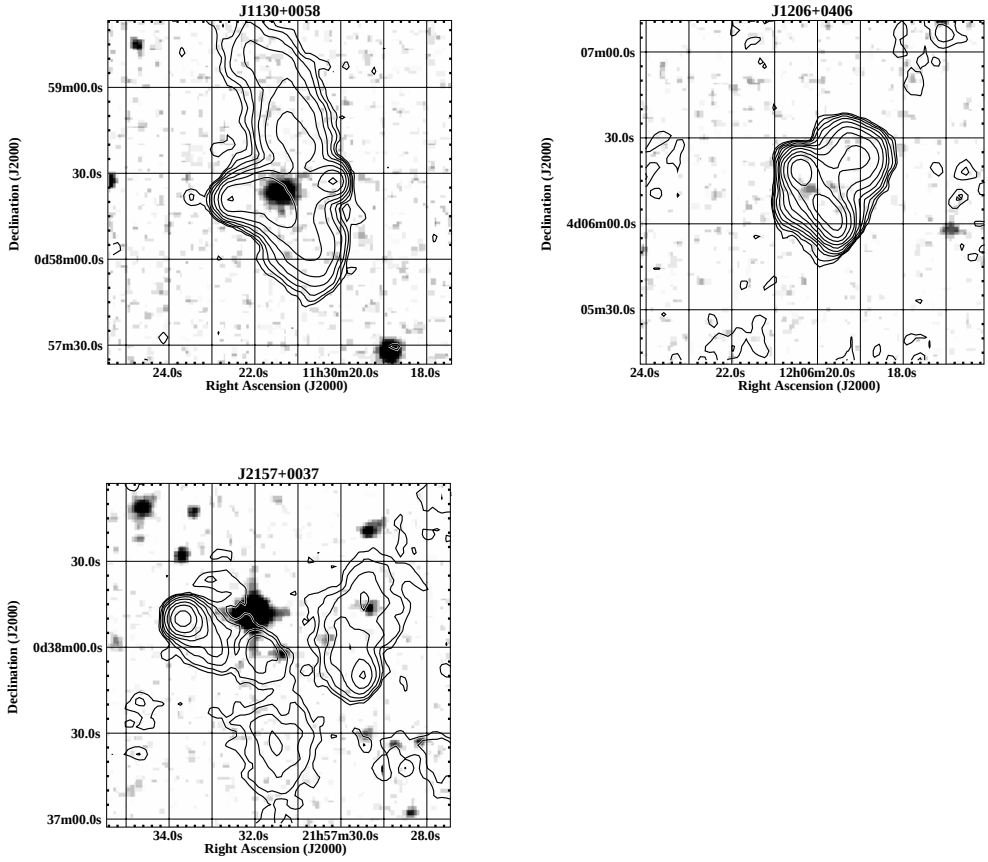

FIG. A5.— As in Figure A4, but for 3 of the X-shaped sources from the literature described in the Appendix.